

TIGRA

The Integrated Geological Risk Assessment

**Hazard zoning methods of snow avalanches,
debris flows and rock falls
Final report**

589210-3

20 november 1997

Client: **European Commission.
Directorate General XII**

Contact person: C.ECCLES
Contract reference: N° ENV-CT96-0262

For the Norwegian Geotechnical Institute

Project Manager:


Karstein Lied

Report prepared by:

Karstein Lied, Ulrik Domaas,
Frode Sandersen, Carl Harbitz

Reviewed by:

Ulrik Domaas



Summary

The present report describes natural hazard zoning methods for snow avalanches in Norway and in some other countries where avalanches are a serious threat to the society. In addition methods for rock-fall and debris slide zoning in Norway are discussed.

The main problem in hazard zoning of avalanches and other kind of natural hazards in steep terrain, is the prediction of the runout distance for a given frequency. To day much effort is put into modelling of avalanche dynamics as the physical processes in avalanches and slides are not fully understood. More research and development is needed to make the models more precise, and to verify the different models towards Nature.

Different kinds of runout models are described in the present report, both empirical/statistical - and dynamical methods.

Hazard mapping legalisation, and mapping procedures are described. The countries included in this overview have all developed national regulations concerning avalanche risk levels. The accepted risk levels differs for all of the countries, as the return periods of the design avalanches ranges from about 150 to 5000 years.

Hazard zoning in Norway is exemplified by a description of a case study in a hazard prone village. The use of a Norwegian GIS system for this purpose is described.



Contents

| | |
|--|----|
| 1 INTRODUCTION..... | 4 |
| 2 HAZARD ZONING PRINCIPLES..... | 4 |
| 2.1 Mapping standard | 4 |
| 2.2 Types of maps..... | 5 |
| 2.3 Zoning procedure..... | 6 |
| 2.4 Detailed maps | 7 |
| 3 HAZARD ZONING IN SOME OTHER COUNTRIES | 7 |
| 3.1 Austria..... | 7 |
| 3.2 Switzerland | 8 |
| 3.3 France..... | 10 |
| 3.4 Iceland..... | 11 |
| 4 LEGISLATION..... | 11 |
| 4.1 Austria..... | 11 |
| 4.2 Switzerland | 12 |
| 4.3 France..... | 13 |
| 4.4 Iceland..... | 13 |
| 4.5 Norway..... | 14 |
| 5 RUNOUT MODELS..... | 15 |
| 5.1 Snow avalanches..... | 15 |
| 5.2 Rockfalls | 29 |
| 5.3 Debris flows..... | 40 |
| 6 CASE STUDY OF NATURAL HAZARD ZONING | 44 |
| 6.1 Main aim. | 44 |
| 6.2 Location, topography and climate of the study area. | 45 |
| 6.3 Recorded avalanches and slides in Geiranger..... | 47 |
| 7 GIS AS A TOOL FOR HAZARD ZONING. | 48 |
| 7.1 General..... | 48 |
| 7.2 Hazard zoning by GIS..... | 48 |
| 8 REFERENCES..... | 49 |

Review and reference document



1 INTRODUCTION

This report presents an overview of natural hazard zoning methods. The main topic is a study of snow avalanche hazard zoning and how this type of zoning is performed in different countries where snow avalanches are a threat to the community. In addition, hazard zoning methods for debris slides and rock falls are presented.

A brief description of legislation concerning natural hazards in different countries is included.

Runout models for different types of slides and avalanches are described. The runout models are both of the statistical - and of dynamical type.

As a practical example of hazard zoning, a locality in a typical natural hazard area is chosen, to illustrate how hazard zoning and risk analysis is performed in Norway.

A GIS/DTM system is used to calculate runout distances of avalanches and rock falls. Hazard zone maps connected to an avalanche and slide database is performed by the GIS system. In addition soil test pits have been analysed to study the frequency of avalanches and slides.

2 HAZARD ZONING PRINCIPLES

2.1 Mapping standard

The principles of natural hazard zoning maps in Norway is described by Hestnes and Lied, and Lied et al., 1989. The Norwegian Geotechnical Institute has conducted hazard zoning of areas exposed to rockfalls and snow avalanches since 1980.

The maps are divided into two categories according to mapping standard:

- detailed maps
- survey maps.

2.1.1 Survey maps

The maps used are standard topographic maps in scale 1:50.000, with contour line distance 20m. Since 1982 the 1:50.000 maps have been available in digital form in Norway, and since then the hazard zoning process has been computerized.



Survey maps are meant to give general information of hazard risks. The production cover a fairly large area in a short time at low costs. It is estimated that each map sheet which covers an area of approximately 600 km², should be evaluated in 4 weeks.

For the purpose of hazard zoning, a digital terrain model TERMOS was developed by NGI in 1984 (Toppe, 1987), and this model has been in use until 1996. In this system, the topographical/statistical model mentioned in section 5.1.1 is combined with TERMOS into a semi-automatic computerized hazard zoning method.

The main advantage with this system is that extensive areas may be surveyed for avalanche danger in a short time. The avalanche runout model used is based on topographical parameters identified by the computer, from the information given in the map.

At present this method of hazard zoning is performed by a commercial GIS system (PUMASTATION), and the commercial digital terrain modelling system SURFER, for the computation of avalanche runout, storage of avalanche data in a relationdatabase, and for the the graphical presentation of hazard zones.

2.1.2 Detailed maps

Detailed maps should have a high degree of accuracy. These maps demand comprehensive field - and computational work and they are time consuming to produce. In Norway such maps are based on the Norwegian economic map series at a scale of 1:5000, contour line distance 5m, or for certain areas in scale 1:1000, contour line distance 1m. In this zoning process each avalanche path is examined in detail; both rupture area, track and runout zone are evaluated carefully, first of all to identify the magnitude, frequency, and runout distance of slides and avalanches.

2.2 Types of maps

Depending on map content and methods used in data collection and data processing, NGI found it appropriate to distinguish between three types of hazard maps:

Hazard registration maps. Maps containing historically known slides and avalanches, compiled from litterature and documents, interviews and field work.

Geomorphic hazard maps. Maps containing information of hazard prone areas identified by geomorphological investigations in the field, and by the use of topographic maps and air photos.

Hazard zoning maps. Maps which define risk areas compiled on the basis of known historic events, geomorphological investigations and the use of frequency/runout calculation models. The hazard zones should correspond to the safety requirements in the national building regulations, or specify other frequency/magnitude conditions of the hazard zone.

2.3 Zoning procedure

2.3.1 Survey maps

As a first step, all potential hazard zones are identified regardless of the frequency of avalanches and rock falls. The hazard zones are divided into two areas:

- Starting zones
- Runout zones.

The starting zones include all areas on the map which are steeper than 30° , and which are not covered with dense forest concerning snow avalanches. Concerning rock fall hazard, all areas steeper than 30° are identified..

The identification of the starting zones are done automatically by the computer, using vector information. On a map sheet with a surface area of 600km^2 this process is completed in 30 minutes.

The runout zones are identified by using the terrain profile in each slide- and avalanche path. Each profile is drawn as a line on the computer screen, from the top of the starting zone, along the path to the valley floor. Based on the information from this terrain profile, the runout distance is calculated by the computer in a few seconds by the topographical/statistical model for snow avalanches and rock falls according to the empirical models described in section 5.1 and 5.2 respectively.

After completion of the hazard map on the computer, the map is checked and corrected by inspection in the field.

Zoning of debris flow hazard has been tried out following the same procedures as for snow avalanches and rock falls. For the time being, NGI's experience is that debris flow hazard is too complicated to be solved in a survey hazard zoning



procedure, as the investigation of this type of hazard needs more basic field work than potential snow avalanche- and rock fall areas need. Hazard zoning of debris slides is therefore performed by detailed zoning procedures only, see sect 5.3.

2.4 Detailed maps

Three different sources of information are used to complete a detailed hazard map:

- records of historic avalanches
- geomorphic analysis of the avalanche path
- computational models for runout calculation.

All information of known avalanches and slides, their runout distance, damage, weather conditions connected to the release etc. are collected. Both oral information and written records are used.

Geomorphological evidence of avalanche frequency and runout is studied in the field. First of all how vegetation is influenced by avalanche activity, and how loose deposits are eroded, transported and accumulated in the avalanche track.

Bedrock type and quality is investigated, together with the distribution of and type of loose deposits.

Debris flow hazard is identified mainly in terrain formations at, and nearby river fans. Earth profiles from test pits are used also to identify and date type and frequency of slides, see sect. 5.3.

Runout models for avalanches and slides are an important tool concerning the establishment of the hazard zones. Each avalanche and slide path is modelled in detail by using digital maps and terrain models. The runout models described in sect 5.1, 5.2 and 5.3 are used to calculate the hazard zones corresponding to the national safety requirements for natural hazards.

Calculation of the runout distance of debris flows have up to present been done manually. The empirical model described in section 5.3 will be computerised during 1997 in the same way as described for snow avalanches and rock falls.

3 HAZARD ZONING IN SOME OTHER COUNTRIES

3.1 Austria.

In Austria and Switzerland every community («Gemeinde»), with avalanche problems has to make a «Gefarenzoneplan» or detailed avalanche hazard map in a scale between M 1:10.000 and M 1:1.000. (Hopf 1990). These maps will give detailed information regarding avalanche and torrents runout zones,

historic records, return periods and/or pressure from the avalanches. Two hazard zones are used:

-Red zone: Avalanche frequency greater than 1/10, or impact force greater than 25 kPa.

-Yellow zone: Avalanche frequency greater than 1/150, and impact force greater than 1 kPa.

The 150 year return period is in most cases a theoretical value, because the length of the appropriate observation periods is too short for statistical analysis. (Sauermoser 1997). For practical purpose, the biggest observed event in the past is therefore the basis for further investigations and often used as the design avalanche.

Based on the information the maps and reports holds, the municipal boards can either avoid planning of new housing areas in avalanche hazard zones or take precautions for new and old living houses situated inside the avalanche zones. This can include physical measures like strengthening the houses with concrete, making deflecting walls or earth dams near the houses, or retaining fences and reforestation in the avalanche release areas. (Domaas 1995).

Prior to accepting a Hazard Zone Plan in Austria the plan is forwarded as a proposal on a official hearing for four weeks in the community before the official commission take the last evaluation of the plan which is thereby stated officially.

It is important to notice that the Austrian Hazard Zone Map take into account the problem of torrent hazard also. (i.e. debris flows).

3.2 Switzerland

Avalanche mapping was started as far as 100 years ago when the Swiss federal forester J. Coaz invited the cantonal forest service personnel to collaborate on the first Swiss Avalanche cadastre (Frutiger 1980). From 1878 - 1895 an avalanche map over Switzerland in scale 1:250.000 was made and publicised by Eidg. Department des Innern, Bern 1907. The maps show each avalanche described by a line from the release areas to the valley. This gives a rough estimate of the limits of the known avalanche events.

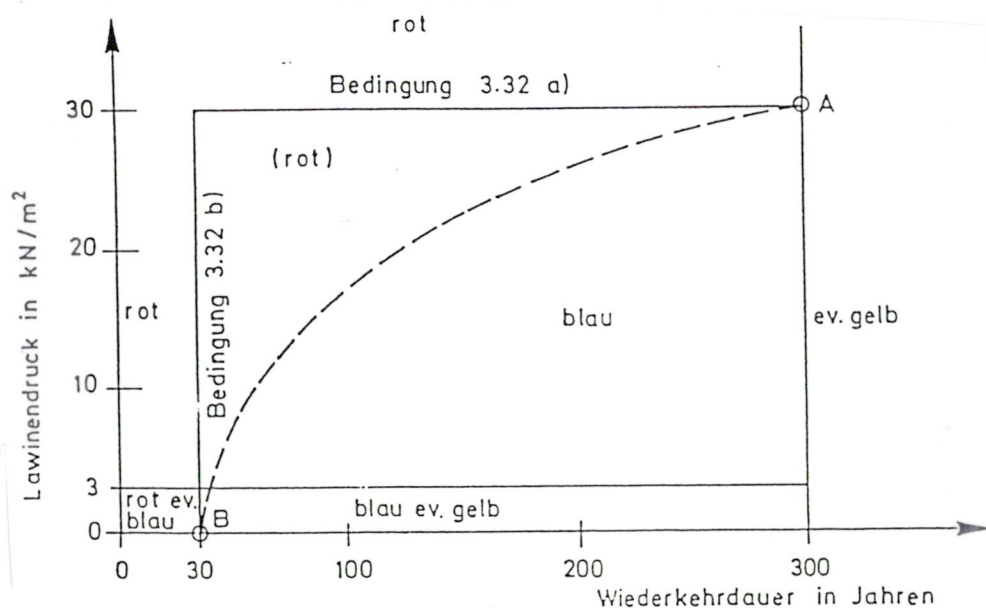
22 avalanche danger maps was later made in scale 1:100.000 by M. Clay and C. Wicki in 1975. The maps show the avalanche danger area and also rockfall and torrents. The maps include known avalanche paths (dark red colour), and for the first time a potential avalanche zone (light red colour). Torrent problem areas is shown with blue lines and dotted lines. These maps is still not very detailed.

In 1978 K. Oechslin made nine detailed maps in kanton Uri in the scale M 1:25.000. On the maps the historic avalanches is drawn with an orange colour, and distinction is made between «Fliesslawinen» and «Staublawinen».

The Eidg. Institut für Schnee- und Lawinenforschung in Davos has made «Winterberichte» each year since 1940. All known avalanches causing material and life losses is reported with known snow conditions.

In the period from 1956-1978 264 internal reports with maps in scale M 1:10.000 is made at EISELF. Avalanche hazard maps is by this made for 26 communities (Gemeinde), and the avalanches on these maps is described with a blue and a red zone, corresponding to the avalanche pressure and the frequency as done in Austria. (Salm 1990, Gubler 1990)

Since the seventies quantitative hazard mapping criteria have been stated. These criteria are based on calculations. The potential hazard is related to the expected frequency, expressed in return periods, and the intensity, expressed by the avalanche pressure, of the avalanche. Combinations of frequency and pressure define the three levels of hazard: High (Red), moderate (Blue) and safe (White). Sometimes a low hazard level (Yellow) is included, namely powder snow avalanches. Avalanches with return periods up to $T = 30$ years mean red zone independent of pressure. For less frequent events with $30 < T < 300$ years a blue zone is applied up to pressures of 30 kN/m^2 . Events of $T > 300$ years are accepted risk (yellow zone).



The Swiss method to distinguish between hazard zones in relation to avalanche pressure and avalanche frequency.

In Swiss avalanche hazard zoning there is an understanding that you can not achieve absolute safety. In the federal Guidelines maximum tolerable risk is given for each zone. With the limitation to consider only events up to 300 years, a generally tolerable risk has been fixed. Principally building is prohibited in the red zone. In the blue zone building is possible, but with caution and provided that certain safety specifications are met. Houses exposed to avalanche forces must be designed to withstand the pressures. In order to minimise the fatalities of an avalanche accident the communities have to organise a warning system and also evacuation of endangered people.

The assessment of tolerable risk is finally a political question. The disaster prevention is a duty of the local communal authority. The communes are theoretically free to make their own risk scale. The only possibility of the confederation to interfere is to reduce the funds for avalanche defence work if the guidelines are disregarded.

3.3 France

The hazard zoning in France is performed by making a Zoning Plan of Avalanche Exposed Areas (P.Z.E.A.) The maps are in scale 1:2000 or 1:5000 and indicate 3 different hazard zones. The maps are made based on the expert's knowledge, and local observations and inquiry. (Borel 1991). The use of runout calculations has been unfrequent until lately, as one lack meteorological data which is needed for the use of the Voellmy-Salm runout model used in Switzerland.

Three different hazard levels are defined according to the following figure:

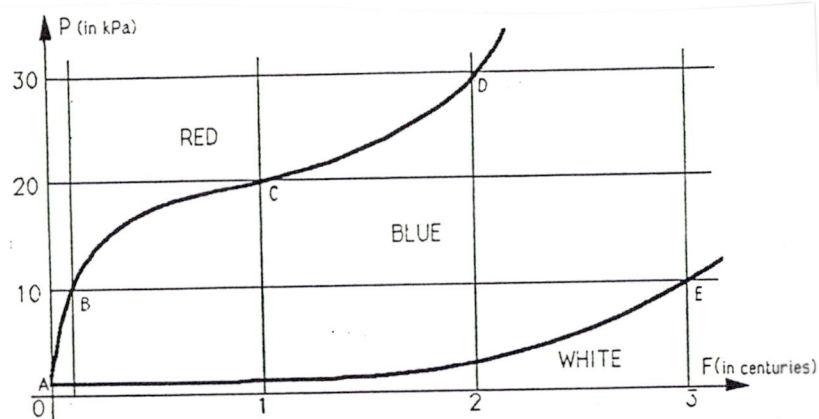


Figure 2. Theoretical P.Z.E.A. zoning diagram (Cl. Charlier, CEMAGREF, 1980)

With :

P : Pressure value

F : Probable period

A (P=1 ; F=0) : Physical limit of the avalanche (doesn't knock down a standing man)

B (P=10 ; F=0.1) : If P > 10 kPa and F probably < 10 years, then : RED

C (P=20 ; F=1.0) : If P > 20 kPa and F probably < 100 years, then : RED

D (P=30 ; F=2.0) : If P > 30 kPa and F probably < 200 years, then : RED

E (P=10 ; F=3.0) : If P < 10 kPa and F probably > 3 centuries, then : WHITE.



3.4 Iceland

Hazard zoning in Iceland was started on a national scale as a result of two major accidents in 1995, when 34 persons were killed in their homes by snow avalanches. Most of the houses were located in areas that were regarded as safe on earlier maps.

The Icelandic aim is to make hazard maps in scale 1:5000 where the actual risk of death for persons staying in a living house is calculated. The acceptable risk lines are drawn on the hazard zoning maps. The models used to calculate the runout distance is both a topographical/statistical model of the same type as developed by NGI (Johannesson 1996), and the PCM model described in section 5.1. By back-calculating avalanche velocities in avalanches which have hit buildings and killed people, it has been possible to find a relation between avalanche velocity and death rate. By combining the runout calculations, velocity calculations, and death rate connected to the velocity, the Icelandic snow avalanche hazard is expressed in the form of a hazard risk map. (Jonasson and Arnalds 1997).

4 LEGISLATION

4.1 Austria

The Federal Service for Torrent and Avalanche Control has existed for more than 100 years, and has been dealing with technical and biological methods against these kinds of natural hazards. In 1975 the institution was authorised by a new Forest Law⁴⁾ with the elaboration of avalanche and torrent hazard maps. These maps are intended to be a base for decisions concerning control measures, regional planning, constructions and safety regulations. (Hopf 1990)

Experts of the Federal Service for Torrent and Avalanche Control (educated at the University of Agriculture and Forestry in Vienna) have to investigate the sources of danger in the catchments and starting zones, taking into consideration hydrological, geological, meteorological, climatic and biological conditions and human influences. Information's about events in the past must be collected. Chronicles and information's of the local people and calculations have to be observed. All the data must be evaluated for the performance of hazard maps. This is also stated in a code for hazard mapping^{5a,b)}.

⁴⁾ Forstgesetz 1975 in der Fassung der Forstgesetz-Novelle 1987

^{5a)} Richtlinien für die Gefahrenzonenabgrenzung. BMLF Referat VC8a Forsttechnischer Dienst für Wildbach- und Lawinenverbauung.

^{5b)} 436. Verordnung des Bundesministers für Land- und Forstwirtschaft vom 30. juli 1976 über die Gefahrenzonepläne.

Beyond this regulation in The Federal Forest Law some executive rules for the hazard zoning are hold in the regional planning laws of the provinces. In the law of the province of Tirol it is stated that areas which are endangered by floods, mudflows, rockfalls, landslides and avalanches are not allowed to be defined as building land. The Ministry of Agriculture and Forestry has decided that in case of non observance of the hazard zone maps, public funds are not available further on, and funds already paid must be reimbursed.

Since protection measures is widely used in Austria it is also of vital interest to know how these measures influence the hazard zones. This is stated in a paper on technical rules for torrents and avalanche protective measures⁶.

4.2 Switzerland

Switzerland is divided in 26 cantons which in turn is divided in several communities. The municipal authority must guarantee the safety of the citizens and property against any kind of danger. This general principle confirmed by the Swiss supreme court (1971) is called the «general police clause». The cantons make the building codes and legislation's themselves, with further details in the legislation's by the communities. By 1980 only six cantons of twelve situated in avalanche districts, had cantonal natural hazard building and zoning codes.

The Federal Forest Law says (Executive Ordinance 1965): «The Confederation cannot subsidise avalanche defences for the protection of buildings or resettlements, if, in selecting building sites, no consideration has been made of the avalanche zone plan and the avalanche cadastre or, if those things are missing, warnings have been disregarded.»

In 1972 The Federal Assembly accepted the Federal Act concerning urgent measures for land-use planning (valid only limited time). After that it must be replaced by a Federal Law.

The Federal Act resolves that: «The cantons, without delay, designate the areas, the use of which is restricted or prohibited for the purpose of the protection of the environment, for recreational purpose, and for protection from natural danger.

The Federal Council supervises the execution of this act. If the cantons do not designate those areas in due course the federal Council will take measures against such cantons.

⁶ Technische Richtlinien für die Wildbach- und Lawinenverbauung. Bundesministerium für Land- und Forstwirtschaft. Ausgabe 1983.



The Federal Act is now replaced by the Federal Law on land-use planning (1980). Art. 6 says: «The cantons designate areas considerably endangered by natural hazards» («considerably» is due to interpretation). This is made by the «Swiss guidelines for Avalanche Zoning (1984)», elaborated by the SFISAR and a Swiss working group. These guidelines has no legal liability, and the cantons are therefor free to have their own guidelines. In general these Federal guidelines are observed by the cantons and communities, also because the Federal Institute in Davos makes consultant work in the communities.

4.3 France

In France «Natural Hazards» were incorporated in the Building code in the same way as the other main land-planning preoccupations. As a general rule, the Mayor and also the State, must ensure the public safety, and make the risk known to the public in the actual Building Documents. (Borrel 1991). The Planning and Building Documents consists of a Land Use Program (P.O.S.) which delineates building areas or zones to be built in the future, and where natural hazards should be taken into account.

As far as the avalanche hazard is concerned, 2 documents must be added to the P.O.S:

- A three colour hazard map which delimits the zones
- The corresponding regulations, which lead either to building prohibition, or to acknowledgement.

For tourist facilities a special Tourist Development Plan (P.D.T.) for mountainous areas must be worked out, including natural hazard assessments.

4.4 Iceland

Icelandic conditions concerning natural hazard legislation are under development, and a draft of natural hazard regulations will be presented to the government during 1997. The regulations will be based on the concept of acceptable risk (Johannesson and Arnalds 1997). This acceptable risk level have been much discussed in Iceland, and the risk value that is considered acceptable will define the limits of the hazard zones. At present, the Icelandic Meteorological Office, which is responsible for the avalanche hazard zoning is using the value $0.3 \cdot 10^{-3}$ per year as the acceptable limit for hazard zoning in living house areas. For comparison, the probability of being killed in a car accident in Scandinavia is about 10^{-4} per year.



4.5 Norway

The Building and Planning Act in Norway has been under development since 1924 and the act was put into force for the whole country in 1966. The last revision was done in 1987. The building act is used when a detailed hazard plan is made with corresponding detailed maps. The ongoing hazard mapping on survey maps M 1:50.000 has been operative since 1979, and up till now approximately 110 maps is finished. Still 100 maps is necessary to prepare and we still need 15 more years to accomplish this work. So far these maps has no legal liability, but will be used as an aid in land use planning in the communities.(Hestnes 1990)

The building council of the communities will have to follow the rules stated in the act, and advises concerning hazard zones and protective measures are done by NGI as a private consultant in each case. In cases where the avalanche endangered houses are older than from 1966, the National Fund for Natural Disaster Assistance can give economical support to rebuild with protective measures or to move the houses elsewhere.

In 1980 a new act became operative in Norway which states that all objects with fire Insurance are also obliged to take out Natural Hazard Insurance. Damages caused by avalanches will normally be compensated in full unless the client has shown gross negligence. However, insurance companies will neither initiate any hazard evaluation nor safety measures. They may, on the other hand, increase the insurance premium or refuse rebuilding. (Hestnes 1990)

The estimation of natural hazards are connected to the Norwegian Planning and Building Law. According to the Technical regulations in the law, three classes of avalanche and slide frequencies are usually taken into account:, se table below.



| Security class | Maximum nominal avalanche frequency per year | Avalanche return period. (years) | Type of construction |
|----------------|--|----------------------------------|--|
| 1 | 10^{-2} | 100 | Garages, smaller storage rooms of one floor, boat houses |
| 2 | 10^{-3} | 1000 | Dwelling houses up to two floors, operational buildings in agriculture |
| 3 | $<10^{-3}$ | <1000 | Hospital, schools, public halls etc. |

In addition, the Building regulation states that rebuilding after fires or other kinds of reparation may be done for class two, when the nominal yearly frequency is less than $3 \cdot 10^{-3}$, i.e. return period of 333 years.

By using the word «nominal», as opposed to «real», one admits that exact calculation of avalanche runout distance for the given frequencies is not possible, and use of subjective judgement is therefore necessary.

5 RUNOUT MODELS

5.1 Snow avalanches

5.1.1 General

Snow avalanches usually starts as a slab, about 0.5 m - 3 m thick. The rupture consists of a tensile failure at the upper boundary, and a shear failure at along a weak layer in the snowpack. The slab may have a width ranging from about 50 m to 1000 m or more, including snow volumes in the order of $10^2 \text{ m}^3 - 10^6 \text{ m}^3$. During the rupture, and shortly afterwards, the slab breaks into blocks which glide at older layers of snow deeper in the snowpack. As the velocity increases, the blocks are broken into smaller pieces, turbulence increases and the movement takes form of a particle flow. In bigger dry avalanches, maximum velocities are about 60-80 m/s.

Most avalanches consist of at least two parts. One is referred to as a dense snow avalanche (or flowing avalanche) which is a gravity flow. The other is a turbidity part referred to as an (airborne) powder snow avalanche, which is driven by the extra weight of small snow particles ($< 1 \text{ mm}$) suspended in the air. A fully developed avalanche can be divided in four flow layers (Norem, 1995a). The major volume of the avalanche is represented by the basal and



liquefied *dense flow layer*, where the particles are in close contact, and the volumetric density is high. The density is assumed to be almost constant. Above the dense flow layer is the transitional *saltation layer*, where the particles are transported in jumps similar to saltating particles in drifting snow. The volumetric density is reduced to the power of three with height in the saltating layer. Then follows the *suspension layer* that constitutes the snow cloud of the avalanche. Here the density and the velocity are both reduced almost linearly with height. Above and around the avalanche is a backflow of air named the *recirculation layer*, with a height one to three times that of the suspension layer. The latter three layers constitute the turbidity part.

Since the material properties differ, the distinction between wet snow (generally cohesive with possible snowball formation) and dry snow (no free water content) avalanches is useful. Dense snow avalanches can occur under both wet and dry snow conditions. A turbidity part is normally generated in both circumstances, especially in steep slopes. Pure powder snow avalanches require dry snow conditions.

Both wet snow and dry snow avalanches involve high internal deformation and are more or less in a liquid state. For wet snow avalanches, solid concentrations are high, and energy dissipation is caused mainly by particle interactions. In dry snow avalanches, energy dissipation is caused mainly by particle interactions at high solid concentrations, and by viscosity in the interstitial air at low concentrations.

The first attempt to formulate a general theory of avalanche motion was made by Voellmy (1955), and this theory is still widely used. Increased human activity in mountain regions, deforestation from pollution, forestry and ski resorts as well as anticipated warming of the earth's atmosphere have caused a growing interest in the study of catastrophic avalanches. Both statistical, and comparative models for run-out distance computations as well as dynamic models for avalanche motion simulations are now developed. However, no universal model has so far been made. The dynamics of avalanches are complex, involving both fluid, particle and soil mechanics. The limited amount of data available from real events makes it hard to evaluate or calibrate existing models. Often several models with different physical descriptions of the avalanche movement can all fulfil the deficient recorded observations.

Material properties, boundary conditions, release mechanisms, impact pressure, defence structures, physical experiments, case studies or other related avalanche topics are omitted in this brief report. For further studies, the following review papers are referred: Hopfinger (1983), Mellor (1978), Norem (1992, 1995a,b), Perla (1980) and Scheiwiller and Hutter (1982).

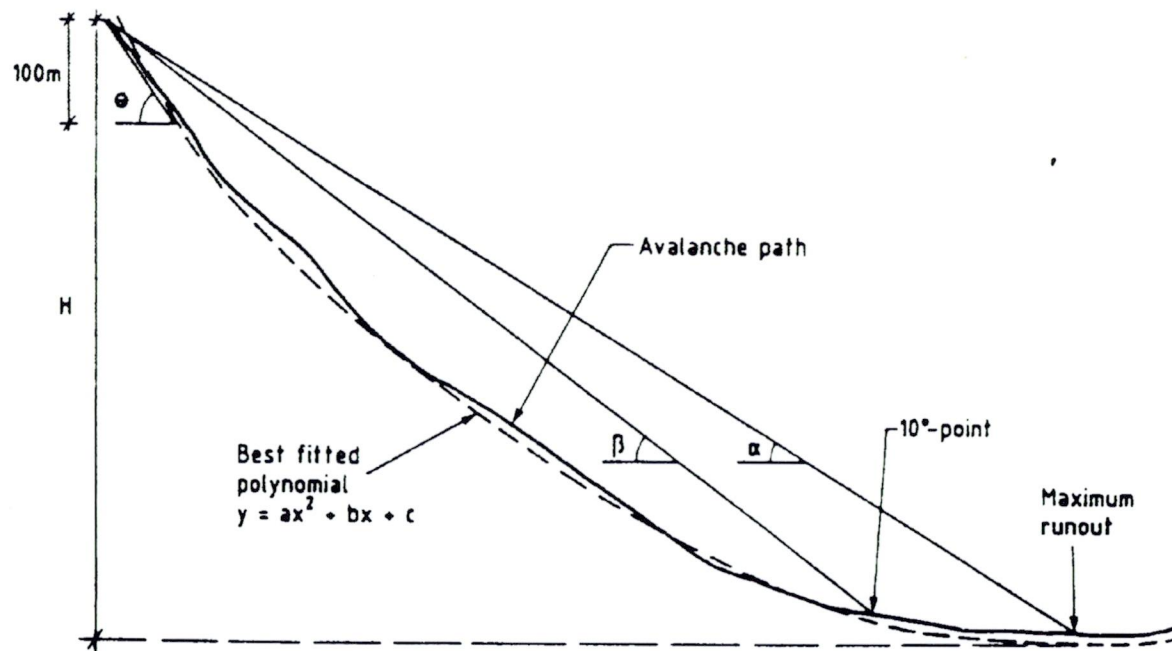


5.1.2 Lied - Bakkehøi statistical α/β -model

The statistical α/β -model (Lied and Bakkehøi, 1980, Bakkehøi et al., 1983, Lied and Toppe, 1988, Bakkehøi and Norem, 1994) was developed at NGI and governs maximum run-out distance solely as a function of topography. The run-out distance equations are found by regression analysis, correlating the longest registered run-out distance from 206 avalanche paths to a selection of topographic parameters. The parameters that have proved to be most significant are:

Topographic parameters governing maximum run-out distance.

| Symbol of parameter: | Parameter description: |
|----------------------|---|
| β (deg.) | Average inclination of avalanche path between starting point and point of 10° inclination along terrain profile. |
| θ (deg.) | Inclination of top 100 vertical meters of starting zone. |
| H (m) | Total height difference between starting point and lowest point of best fit parabola $y=ax^2+bx+c$. |
| y'' (m^{-1}) | Curvature of avalanche path. |



Topographic parameters describing terrain profile (after Lied and Toppe, 1988).

The β -angle is empirically found to be the best characterisation of the track inclination.

The inclination θ of the top 100 vertical metres of starting zone indirectly governs the rupture height, and thereby the slide thickness, which is greater in gentle slopes than in steep slopes. Hence smaller values of θ give longer run-out distances or smaller average inclination of the total avalanche path, α .

In Norway most avalanche paths might be approximately described by the parabola $y=ax^2+bx+c$, of which curvature is described by the second derivative $y''=2a$.

In slide paths with little difference in height, H , a smaller part of the potential energy is transformed into heat by friction. Hence the avalanches have an apparently lower coefficient of friction, and obtain theoretically a smaller run-out angle.

For a parabolic slope, the β -angle is determined by $\beta = \tan^{-1}\left(\sqrt{\frac{Hy''}{2}} + \frac{\tan 10^\circ}{2}\right)$.

Smaller values of the product Hy'' mean smaller values of β . This results in smaller values of α , because the avalanches run with smaller velocity, and the velocity-dependent frictional transformation of potential energy into heat is reduced.



The topography, the width and the degree of lateral confinement in the starting zone, as well as the drifting snow transport into the starting zone, have little influence upon the run-out distance (Lied and Bakkehøi, 1980, Lied et al., 1995). As opposed to what was presumed, no tendency was found that an avalanche with a wide rupture zone, which is channelled into a narrow track, has a longer reach than an avalanche following an unconfined path.

The regression analysis revealed that the β -angle is the most important topographic parameter. The result of the regression analyses is referred in the table below:

Results of regression analysis (translated from Bakkehøi and Norem, 1994, with standard deviations (SD) and correlation coefficients (R). [H] represents the numerical value of H.

| Assumption | No. of avalanches | Regression equation, $\alpha=$ | Accuracy | | Standard deviation (m) H=1000m, horizontal run-out | | |
|--|-------------------|---|--------------|----------|---|--------------------|-------------------|
| | | | SD (deg.) | R [-] | α (deg.) | $-\Delta L$ (m) | ΔL (m) |
| $\beta \leq 30^\circ$ | 68 | $0.89\beta + 0.035\theta - 2.2^\circ \cdot 10^{-4}[H] - 0.9^\circ$ | 1.49 | 0.84 | 25 | 138 | 154 |
| $30^\circ < \beta \leq 35^\circ$ | 59 | $1.15\beta - 2.5^\circ \cdot 10^{-3}[H] - 5.9^\circ$ | 2.50 | 0.53 | 30 | 162 | 189 |
| $\beta > 35^\circ$ | 79 | $0.81\beta + 0.036Hy''\theta + 3.2^\circ$ | 2.67 | 0.62 | 36 | 127 | 144 |
| $\beta \leq 30^\circ$, H \geq 900m | | $0.94\beta + 0.035\theta - 2.6^\circ$ | 1.02 | 0.90 | 25 | 96 | 103 |
| All avalanches | 206 | $0.96\beta - 1.4^\circ$ | 2.30 | 0.92 | | | |
| All avalanches | 206 | $0.92\beta - 7.9^\circ \cdot 10^{-4}[H] + 0.024Hy''\theta + 0.04^\circ$ | 2.28 | 0.92 | | | |

The model is most appropriate for travel distance analysis along longitudinally concave profiles. The calculated run-out distances are those that might be expected under snow conditions favouring the longest run-out distances. The authors have no explanation as to why there is such a small correlation in the data for $30^\circ < \beta \leq 35^\circ$.

Lied and Toppe (1988) redefine the starting zone as the part of the path lying between the starting point and the point of 30° inclination along the terrain profile. The average inclination of this zone is termed γ . They further describe the automatic computation of the avalanche parameters. Applying the relation $\alpha = f(\beta, \gamma)$ for 113 avalanches, the equation $\alpha = 0.91\beta + 0.08\gamma - 3.5^\circ$ gives $R^2=0.94$ and $SD=1.4^\circ$, which is a small improvement to the relation between α and β in Table 2.2. Lied and Toppe (1988) also present combinations of the lengths of the starting zone, the avalanche track and the run-out zone, L_1 , L_2



and L_3 respectively as well as the area A of the starting zone (evaluated subjectively from local topography as a substitute for the avalanche volume). The best relation is $L \equiv L_1 + L_2 + L_3 = 0.93L_1 + 0.97L_2 + 0.61m \cdot [A] + 182m$, with $R^2=0.96$ and $SD=137m$ ($[A]$ represents the numerical value of A [m^2]). Using L_3 alone as the dependent variable does not give R - and SD -values that enable sufficiently accurate calculations of run-out distance. The prediction of path lengths will give run-out distances independent of steepness of path, as opposed to the more realistic α/β -relations. McClung and Lied (1987) show that the avalanches with the 50 highest values of the ratio $L_3 / (L_1 + L_2)$ give a very good fit to an extreme-value distribution.

The assumption of small variations in the physical snow parameters giving the longest run-out distance is only valid within one climatic region (McClung et al., 1989). Martinelli (1986) and McClung et al. (1989) have applied the basics of the statistical α/β -model in mountain regions outside Norway.

The avalanche database of NGI is constantly extended, and contains at present 230 events. Both the statistical and the dynamic models are occasionally recalibrated.

5.1.3 Voellmy block model

Voellmy's (1955) model is a one-dimensional block model for the calculation of avalanche run-out distance.

The sliding mass is considered as an endless fluid of height H reaching a terminal velocity by equilibrium of gravitational forces and shear forces on an infinitely long slope of constant inclination θ_1 . Based on hydraulic theory, the shear forces are represented by a dynamic drag proportional to the terminal velocity squared on the free, upper surface and a combination of a similar dynamic drag and a Coulomb friction proportional to the normal forces along the bed. Hence the terminal velocity is expressed by the two-parameter formula

$$V_t = [\xi H (\sin \theta_1 - \mu \cos \theta_1)]^{1/2}$$

where density and drag coefficients are lumped together into the «coefficient of turbulent friction», ξ [m/s^2], and μ is the Coulomb friction coefficient. To account for lateral confinement, H is replaced by the hydraulic radius (flow cross-sectional area divided by wetted perimeter).

The deceleration starts at a certain reference point, normally located where the actual slope inclination equals $\tan^{-1}\mu$. From this point the run-out distance on a slope of constant inclination θ_2 is computed by energy considerations:



$$S = V_t^2 [2g(\mu \cos \theta_2 - \sin \theta_2) + V_t^2 g / (\xi H_D)]^{-1}$$

H_D is the mean depositional depth accounting for the energy loss due to pile-up of debris and g is the acceleration of gravity.

The computed run-out distance is based on the assumption that terminal velocity is reached, and depends strongly on the selected location of the reference point, as well as on the values of the input parameters.

The values of μ and ξ are discussed by Buser and Frutiger (1980) and by Martinelli et al. (1980).

5.1.4 PCM Block model

The 2-parameter PCM-model (Perla, Cheng and McClung, 1980) is a further development of Voellmy's model above. The avalanche is described as a one-dimensional block of finite mass moving on a path of varying curvature. The reference point is the initial rest position of the block's centre of mass. The equation of momentum includes Coulomb friction, centrifugal force due to curvature of the path, dynamic drag and inertia resistive ploughing. The Coulomb friction term consists of an adjustable friction coefficient μ multiplied by the normal force along the bed. The latter three terms are all proportional to v^2 , the tangential velocity squared, and hence lumped together into one term consisting of v^2 divided by the second adjustable parameter interpreted as a mass-to-drag ratio, M/D [m^{-1}]. The result is a linear differential equation in v^2 :

$$\frac{1}{2} \frac{dv^2}{ds} = g(\sin \theta - \mu \cos \theta) - \frac{D}{M} v^2$$

where θ is the local inclination, s is the slope position and g is the acceleration of gravity. However, the inclination and perhaps the adjustable parameters are not constant along the path. An iterative solution procedure is described, dividing the slope into small segments of constant inclination and parameter values. To compensate for the absence of curvature along the linear segments, the velocity is corrected for conservation of linear momentum at each segment transition.

The usefulness of the model depends on a knowledge of the two adjustable parameters that can vary considerably, cf. Table 19.1. For avalanches, these values have been limited to some extent by testing the model statistically on 136 extreme paths in Northwest USA and Norway (Bakkehøi et al., 1981) and on 206 extreme paths in Norway (Bakkehøi et al., 1983).



Alean (1984, 1985) has analysed nineteen ice avalanches to establish parameter values and test whether the PCM-model might be applicable for such events. He concludes that deviations between model predictions and observations are «disappointingly high», and that a one-parameter model leads to only slightly worse predictions of run-out distances for ice avalanches.

For constant inclination and parameter values along an infinitely long slope, the result is analogous to that of Voellmy.

5.1.5 VSG- refined block model

The VSG-model (Voellmy, 1955, Salm et al., 1990, Salm, 1993 and Gubler, 1993) is the most commonly used model for calculation of avalanche motion in Switzerland and Austria.

The model assumptions are incompressibility of flow along the whole path, steady flow and small variations of flow height along the track (i.e. between starting and run-out zones) and non-steady quasi-rigid body movement in the run-out zone. The model is quasi two-dimensional as it to some extent incorporates the average width of the starting zone, the track and the run-out zone separately, as well as the cross-sectional shape of the track.

The computed velocity v_0 of the mass centre leaving the starting zone is computed in correspondence with the terminal velocity of Voellmy's model (for avalanches a default value of initial flow height d_0 is presented based on statistical analysis of precipitation data from Swiss mountain areas). Given the width of the starting zone, W_0 , the model computes the flow rate $Q = W_0 d_0 v_0$.

The terminal velocity at the bottom of the track

$$v_p = \left[\frac{Q}{W_p} \xi (\sin \psi_p - \mu \cos \psi_p) \right]^{1/3}$$

is based on the average width W_p of a «control section» of a few hundred meters (theoretical length is suggested in Gubler (1993)) at the lower end of the track, μ and ξ are the same coefficients as in Voellmy's model, and ψ_p is inclination of control section. For laterally confined tracks the terminal velocity is given by

$$v_p = \left[R \xi (\sin \psi_p - \mu \cos \psi_p) \right]^{1/2}$$

where R is the hydraulic radius. Dynamic pressure on obstacles along the track is calculated.



The run-out zone is said to begin where the inclination equals $\tan^{-1}\mu$. (Thus the run-out zone starts on more gentle slopes for larger avalanches because the assumed μ values are smaller). By time-dependent modelling of the movement of the avalanche front, and assuming a linear decrease of the velocity squared

$$v^2 = d_s \xi (\mu \cos \psi_s - \sin \psi_s)$$

in the run-out zone of average inclination ψ_s , the length of the run-out zone is

$$s = \frac{d_s}{2g} \ln \left(1 + \frac{v_p^2}{v^2} \right)$$

where g is the acceleration of gravity and deposit height $d_s = \frac{Q}{W_p v_p} + \frac{v_p^2}{4\lambda g}$.

The internal friction parameter of the avalanche mass, λ , determines the transfer of kinetic energy (particle speed) to potential energy (flow height). According to Harbitz (1995), the model results are not very sensitive to the value of λ (equals 2.5 for wet, dense snow avalanches). The run-out zone might be divided into small segments for altering the parameter values and computing the velocity along the slope. The numerical program returns both the limit of the red zone (i.e. where the dynamic pressure exceeds 30 kPa) and the total run-out distance.

An alternative run-out model is also included (Salm, 1993), applicable when there is no enlargement of the flow width in the run-out zone. Now the flow is modelled as a flexible sliding sheet with high internal friction. The model results in lower (more realistic) deposit heights and a faster decrease of flow speed in the run-out zone. This run-out model is more dependent on the value of the internal friction parameter (Harbitz, 1995).

The results of the VSG-model are critically dependent on the input values of width, length and inclination of the starting zone, initial flow height h_0 , friction coefficients, cross-section of the track and inclination of the track and the run-out zones, cf. Table 19.1. A default value of the initial flow height is presented according to the Swiss guidelines (Salm et al., 1993), based upon the altitude of the fracture line, the return period of the avalanche and the climatic region.

The model has been tested for avalanches by Buser and Frutiger (1980), Föhn and Meister (1982), Gubler (1987) and Lied et al. (1995). The latter concluded that the uncertainties for the VSG-model are as great as for the PCM- and NIS-models.



5.1.6 NIS visco-elastic plastic deformable body model

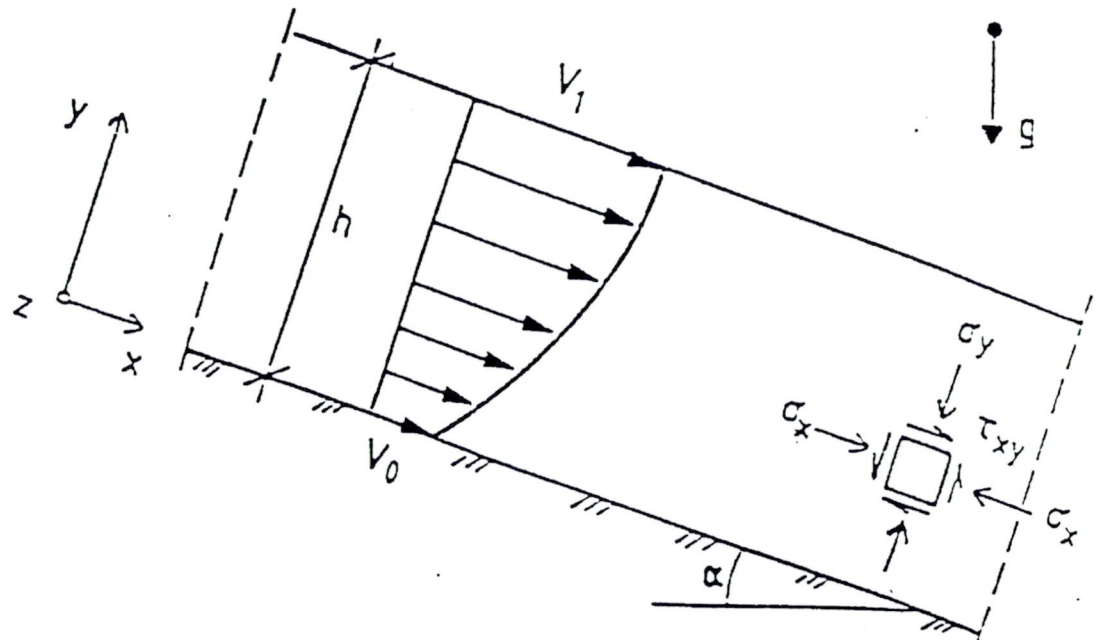
The dynamic model developed by NGI; the NIS-model, (Norem, Irgens and Schieldrop, 1987, 1989, Norem and Schieldrop, 1991), was originally developed for avalanches and has also been applied to submarine flowslides. Thus it is constructed to treat both kinds of energy dissipation regimes outlined in sections 1 and 10. The mathematical deformable body model describes a two-dimensional, non-steady shear flow of varying height with slip velocity conditions when erosion is omitted, or with no-slip velocity conditions when erosion is included. The shear flow moves along an arbitrary path originating centrifugal forces. The constitutive relations, which contain the visco-elasticity of a CEF-fluid (Criminale-Ericksen-Filbey, 1958) combined with plasticity for a cohesive material, yield (as depicted in Fig. 12.1) for the normal stresses σ_x and σ_y parallel and normal to the slope respectively, and for the shear stress τ_{xy} :

$$\sigma_x = p_e + p_u - \rho (v_1 - v_2) \left(\frac{dv_x(y)}{dy} \right)^r$$

$$\sigma_y = p_e + p_u + \rho v_2 \left(\frac{dv_x(y)}{dy} \right)^r$$

$$\tau_{xy} = a + p_e \tan \varphi + \rho m \left(\frac{dv_x(y)}{dy} \right)^r$$

where p_e is the effective pressure (all normal compressive stresses have a positive sign according to soil mechanic practice), p_u is the pore pressure, ρ is the average density of the flowing material, v_1 and v_2 are the normal stress viscosities, $dv_x(y)/dy$ is the shear velocity parallel to the slope at a height y above the bed, a is the cohesion, φ is the internal friction angle, m is the shear stress viscosity and r is an exponent preliminary suggested equal to 2 for rock slides and avalanches (inertial regime) and 1 for debris flows of low concentration and submarine flowslides (macro-viscous regime).



Definition of steady flow geometry (after Norem, Locat and Schieldrop, 1989).

As the viscometric functions are represented by power laws, they express flow induced dispersive pressure and dynamic shear, as described by Bagnold (1954). The model is quasi two-dimensional as the vertical velocity profile is assumed to be identical in form to the steady shear flow profile. Cohesion and/or upper surface shear stress induce a plug flow velocity profile, as opposed to the parabolic flow profile of a non-cohesive material with zero shear stress along the upper surface.

Cohesion, upper surface shear stress and erosion are omitted in the numerical model. The resulting partial differential equations are solved by a Eulerian finite-difference mid-point scheme in space and a fourth-order Runge-Kutta procedure in time.

The rear and frontal grid cells in the finite-difference representation of the avalanche are considered equal to the other cells in between. Each time the accumulated volume (i.e. volume flux integrated in time) passing through the contemporary avalanche front (i.e. the foremost «wall» of the frontal grid cell) matches the volume of the grid cell ahead of the avalanche (i.e. product of



contemporary avalanche front height and grid distance), the avalanche is said to advance one grid distance. Similarly the rear grid cell is empty and neglected when the accumulated volume flowing out of the cell equals the volume contained in the cell when it was first defined to be the rear one, as the one behind was emptied.

To simplify comparison with other models, four program options are implemented:

- varying flow height and slip velocity conditions
- varying flow height and no-slip velocity conditions
- varying flow height and uniform profile
- constant flow height and velocity profile

The latter is approximately equal to the Voellmy or PCM models.

Several input parameters are needed: most important are the material friction coefficient (equals $\tan\phi$) and the initial flow height h of the avalanche, cf. Table 19.1. For avalanches a default value, h_{crit} , is presented for the latter (Bakkehøi and Norem, 1994), based upon the fact that an unstable situation occurs when the actual shear stress, $\tau = \rho g h \sin\theta$ equals the yield strength, $\tau_y = a + \tan\phi \rho g h \cos\theta$, of the snow:

$$h_{crit} = \frac{a}{\rho g (\sin\theta - \tan\phi \cos\theta)}$$

where g is the acceleration of gravity and θ is the slope angle. The cohesion is eliminated by introducing a known reference height, $h_{40}=1.3\text{m}$, for a slope angle of 40° :

$$h_{crit} = h_{40} \frac{\sin 40 - \tan\phi \cos 40}{(\sin\theta - \tan\phi \cos\theta)}$$

A value of $\tan\phi=0.3$ ($\phi=17^\circ$) is applied in the computations.

Bakkehøi and Norem (1994) also suggest that the length of the initial avalanche slab should equal one sixth of the total height difference of the slide path, with a maximum of 100 m.

The numerical results are verified by comparing with laboratory (Norem et al., 1992) and full-scale experimental data of avalanches (Norem, Irgens and Schieldrop 1989, Norem, 1992b), submarine slides (Norem, Locat and Schieldrop, 1989) and rock slides (Locat et al., 1992). For avalanches and submarine slides, the front velocity and the run-out distance are simulated well by the model. With varying flow height, the program is less sensitive to the



shape of the path, and the computed deposits in the run-out zone also agree fairly well with experimental data.

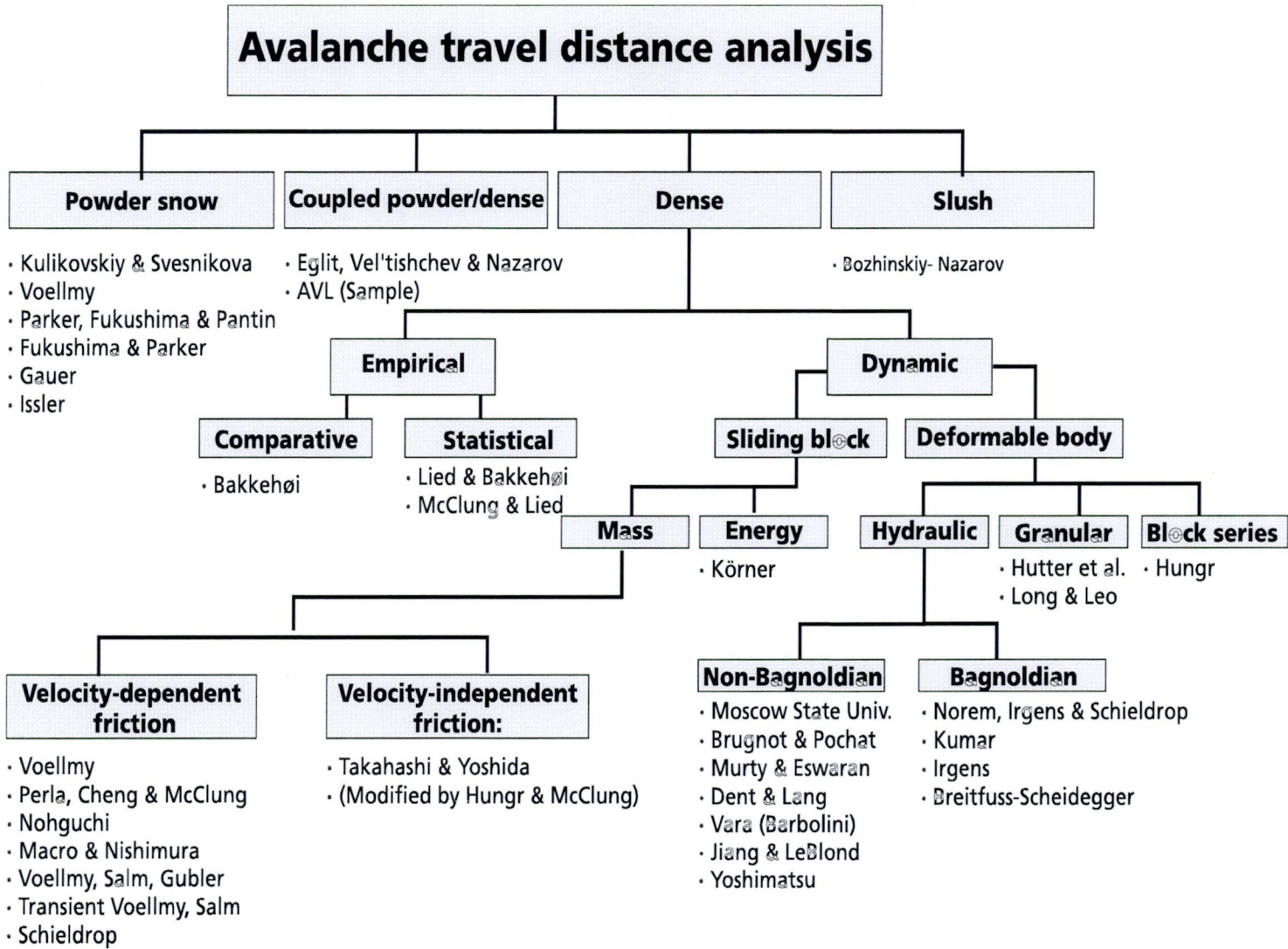
It is an admitted weakness by the authors that the model does not include effects of temperature and volume changes due to altering arrangements of the grains. Neither is the effect of active and passive earth pressure included. However, this effect is probably not significant as the internal friction is low due to the dispersive stress (Norem, pers. comm., 1995).

For hazard zoning purposes it seems that the following models are in use:

- 1) Lied-Bakkehøi statistical α/β - model
- 2) Voellmy block model (VSG-version)
- 3) PCM block model

Most of the other models described in this report need to be verified before they are applicable in snow avalanche hazard zoning.

On the following page an overview of the different models for snow avalanche runout (travel distance) are illustrated.





5.2 Rockfalls

A rock fall is defined as a limited volume of rock masses set in rapid motion on an inclined slope. Rock falls and rock slides are usually classified according to the volume of the sliding masses:

| Type: | Volume (m ³) |
|-----------------|--------------------------|
| Rock falls | <100 |
| Rock slides | 100-10.000 |
| Mountain slides | > 10.000 |

Usually the frequency of rock falls in a given area are considerably higher than the frequency of rock slides and mountain slides. Rock falls usually consist of a limited number of rock blocks that glides, rolls or jumps downhill. The release normally occurs in rock cliffs, steeper than 30°, along joints in the rock mass.

Experience has shown that accurate stability calculations of fissured rock masses is difficult. Very often a complex system of joints are found, where the most important parameters as joint roughness, joint hardness, joint friction and joint water pressure all are difficult to establish. The most critical factor concerning stability calculations are the hydrostatic pressure on fissures, and whether fissures in the bedrock are drained or not. Rock masses which are quite stable during dry conditions may be unstable during conditions with relatively small hydrostatic pressures. Such pressures are difficult and costly to measure in the field.

Another factor of importance is the fact that major mountain sides with vertical drops in the order of 500-1000 m consist of numerous fissured parts where access is limited, and consequently a detailed stability analysis is very time consuming.

Because of the difficulties of performing accurate and reliable stability calculations in such locations, it might be a better way of treating the rock fall hazard, a priori, to admit that rock falls will occur in the future. Instead of trying to calculate stability, it is better to calculate runout distance, and if possible, the frequency of rock falls reaching a given point in the runout zone.

In each of the rockfall cases compiled by NGI, the geometry of the mountainside with release area (the uppermost cliff), the steep area down to the talus or scree, the talus itself with top and toe, and the area beneath the toe of the scree were studied in detail. In order to compare the different cases it has been necessary to make simplifications of the geometry of the mountainsides, as well as leave out the special cases where special topographic features dominates the result.

The analyses show that although there are considerable variations among rockfalls, there are none the less limits to how far blocks can travel. There are

always several reasons for rockfalls not reaching as far as theoretically possible. The results can simply be used as references for own assessments. The runout of blocks rolling and bouncing in steep terrain beyond the talus toe is of particular interest.

In further work on rockfalls, model and full-scale experiments can probably be expected to yield the most useful results. Most of the necessary work on theoretical modelling of rockfall behaviour are presented in papers available. Resistance to rolling and loss of energy through impact have been made the object of simple assessments, and it will probably be possible to assign figures to these parameters through experimental work.

A numerical calculation model has been developed on the basis of a method for calculating the longest run-outs. The model will provide values for the location and design of protective measures. By comparing these values with an assessment of the range, we can obtain realistic values for velocity and run-out distances.

5.2.1 Short review of recent literature on models for the calculation of rockfall movement

A. Ozone (1993) gave a short description of 17 different models concerning kinematics, lumped mass and rigid body mechanics in his thesis leading to his Master Degree. Here we give a short review of these models as well as additional Norwegian approaches and some other important papers on this issue:

Banks and Strohm (1974). The model consider the kinematics behaviour of a discontinuous body sliding on plane segments and calculates velocities and acceleration.

Pieta and Clayton (1976). This model is the first computer program for rockfall analysis. The model considered the rock as a point bouncing and rolling on slope segments with different inclinations. The method take into account rolling and uses restitution and friction coefficients.

B. Schieldrop (1977). The kinematics model describe a point of mass falling on an inclined path and take into account the normal restitution coefficient. The model is later refined and take into account the energy equation, the angular momentum and the moment of inertia. The calculations give the maximum length of the trajectories.



Hestnes, Schieldrop (1977). Rock fall testing on a 50 m long steep 27° slope giving velocities, friction coefficients and understanding of rock fall behaviour. Hacar, Bollo and Hacar (1977). A 2D-model using fundamental equations of cinematic. The method can model all types of movement and take into account the centrifugal force.

Paiola (1978, Bertozzi and Broili (1978) and Focardi (1982). Paiola and Focardi proposed to assess the design parameters of defence structures by back calculating rockfall events. The method can give relevant values for velocity, run-out distance and energy. Bertozzi and Broili assessed restitution and dynamic friction coefficients on a scree under a steep wall and compared this to their kinematics analysis.

Azimi (1982). The model analyse trajectories and energies of falling blocks, related to geometrical and geotechnical characteristics of the topographical surface. The method use a statistical approach.

Bosco and Mongiovi (1986). The model assess the risk of rockfalls. Hoek (1987). A computer program was developed to calculate the bouncing movement without rolling, rotation and sliding.

Hungr and Evans (1988). The analytical model is based on the concept of a energy head reduced by impacts (restitution coefficient) and rolling resistance. A relationship is found between energy, slope geometry and type of motion.

Marie (1988). The method presents a statistical rockfall analysis, where all the parameters are described statistically.

Paronuzzi (1989). The model is a probabilistic approach generating random values of impact, determining the frequency distribution of the kinematics design parameters for a simulated trajectory sample. The model verifies the increase of safety of an area as a consequence of a particular barrier construction.

Falcetta (1985). The model is based on the fundamental laws of dynamics and consider the mechanics of the rigid body. The model is a step by step procedure taking into account the position of the block and the shape of both block and slope at impact. In 1987, the authors proposed a statistical approach based on the same model.

Bozzolo and Pamini (1986). This is a model based on the mechanics of the rigid body (MASSI 1987). The blocks are modelled as ellipsoids and the motion consists of free fall and impact in combination. This give a possibility to model all typical movements. In addition the model can calculate rolling and sliding.



Descoudres and Zimmermann (1987). This is the most complete model and is a statistical three-dimensional model based on rigid body mechanics. The blocks are ellipsoids or prisms and the slope have inelastic or plastic behaviour and with surface roughness.

Spang and Rautenstrauch (1988). The model is based on the rigid body mechanics and the paper presents a comparative review of two- and three-dimensional analysis models, and some sensitive criticisms to the model (1988 and 1991). The method is similar to that of Bozzolo and Pamini.

Pfeiffer and Bowen (1989). This model is also called the Colorado rockfall Program and give a statistical analysis of rockfall simulations. Input values are slope and rock properties and applies equations of gravitational acceleration and conservation of energy to describe the motion of the rock. Empirical derived functions are also used.

Smith and Duffy (1990). Field test measurements of velocity, kinetic and angular energy, and evaluation of rockfall restraining nets.

Larsen (1993). Practical application of the Colorado rockfall Simulation Program.

Domaas U. (1994). The model describe the use of topographic parameters in recorded rockfalls to calculate the runout distance.

5.2.2 Empirical models

The following empirical models are the basis for rock fall hazard zoning in Norway, and described in more detail by Domaas (1994).

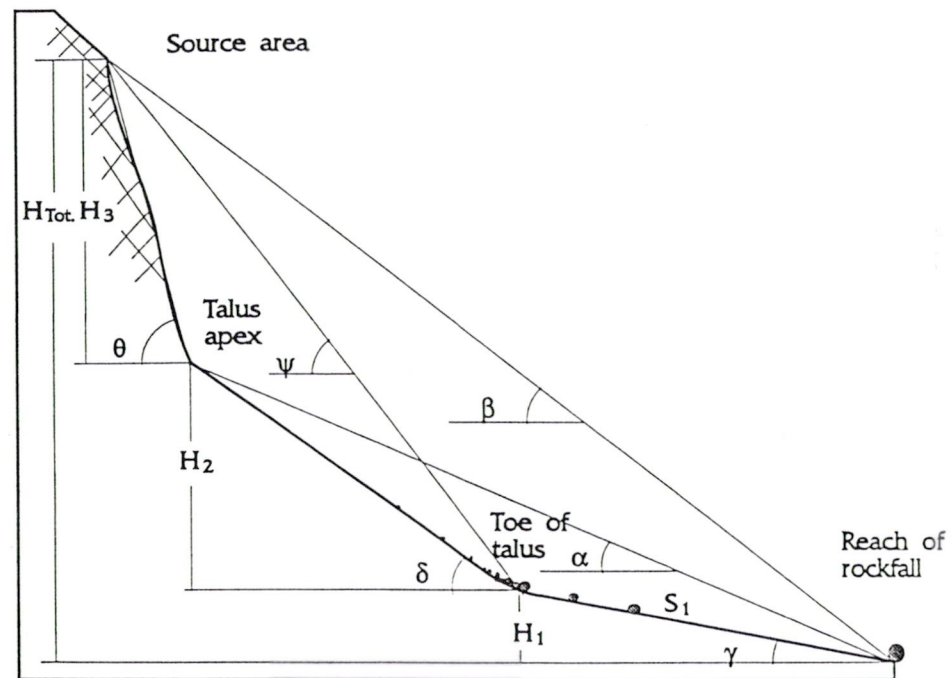
5.2.2.1 Maximum rockfall range related to the height of the mountain side

The potential of falling rocks to run out for long distances is normally expected to depend on the height of the slope. This is reasonable, because the velocity of a rock must increase with the height of free fall. A number of factors affect and complicate the analyses, because the blocks stop at varying distances beyond the talus, and the measured run-out distances therefore show a certain spread. Some of the reasons for this are: the blocks travel across different substrates, which cover a great variation in softness which give the blocks different energy losses in each impact (expression for the percentage of energy recovered after an impact). Blocks may shatter in impact against the substrate, and they vary in shape and size.

All these factors have some effect on the individual block, and make it difficult to quantify the energy losses. Collecting a large number of block registrations from

rockfalls will therefore gradually make it possible to design an outer bound for how far falling blocks can travel in relation to the height of the mountainside.

Analytical work was made difficult by the fact that there was one dominant factor controlling rockfall range. This was the slope of the terrain beyond the talus toe. To make the analyses possible we restricted the analyses to rockfall cases where the average slope was less than 12° beyond the talus toe.



Topographical parameters measured on the terrain profiles.

The height of mountainsides is expressed as the total vertical difference in altitude between the uppermost scarp on the mountainside and the block location (H_{TOT}). The range of the blocks (S_1) is measured from the talus toe. The talus toe or the base of the talus is defined as the lower boundary of the area completely covered by debris. Subjective evaluations of the position of the talus base are unlikely to result in differences of more than a few meters. A bound for 98% of the measurements collected can be expressed by means of the following linear equation:

$$S_1 = a \cdot H + b = 0.3065H_{TOT} + 24.1 \text{ m}$$

In order to include all the measurements, 54.1 m must be used instead of 24.1 m. This is because two blocks showed an extreme reach 30 m farther than the others.



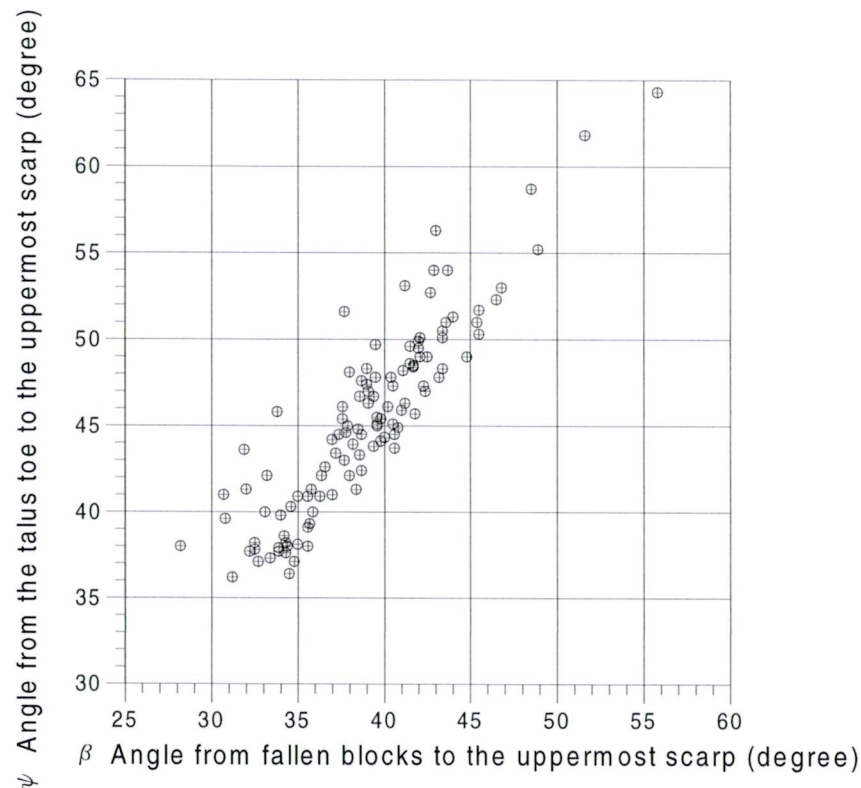
5.2.2.2 Rockfall range described in terms of the angle from the fallen block to the top of the uppermost scarp in the mountainside

The angle β forms what we can call an all-embracing angle which describe the maximum run-out of blocks in a particular mountainside. This angle is also used by Scheidegger (1973) as a basis for a description of the extension of an average friction coefficient (f) for land slides. With respect to the individual blocks, $\tan(\gamma)$ can be physically called the average friction parameter that determines the maximum run-out of a block. In Scheidegger's model, the f -values decrease with increasing volume.

As a general rule, $\beta = 30^\circ$ has been used to give an estimate of the run-out distance for rockfalls. The results show that β depends on the height of the mountainsides. In general, β values are greater than 31° for mountainsides with heights from 100 m up to 350 m. Thereafter the value of β increases linearly up to 35° for mountainsides 650 m high.

5.2.2.3 Rockfall range described in terms of the angle from the talus toe to the top of the uppermost scarp on the mountainside

The height of the mountainside, and the talus height can be used as a basis for determining how far rockfalls can reach. One way of describing the size and shape of the mountainside is by means of angle Ψ , which is measured from the talus toe to the top of the uppermost scarp on the mountainside. 75% of the measurements were from mountainsides that were less than 200 m high.. Although increasing heights can be expected to result in rockfalls with higher velocities, the loss of energy due to impact also increases with height. The relative difference in run-out distance will therefor be somewhat smaller than the difference in hight would seem to indicate. Ψ is a parameter which describes how steep the mountainside is, irrespective of the height of the mountainside. In the figure below, the relationship between the Ψ values is compared with β , so that we get a new expression for rockfall range related to the geometry of the mountainside. The figure shows a close relationship between the two parameters. The fact that the difference between the two angles is normally less than 10° also is important here.



Range described in terms of angles β and Ψ

In order to investigate which effect the vertical drop may have in this context, the measurements are grouped into three height intervals. For practical reasons, the heights are divided into three groups in Figure 5:

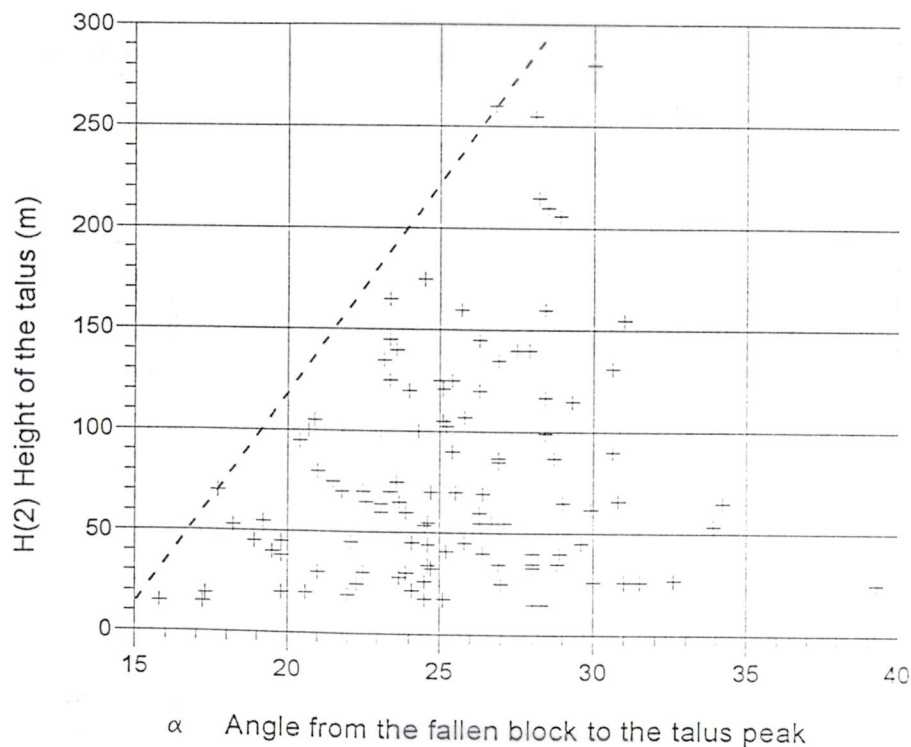
In Figure 5 a tendency can be seen for β values to increase with increasing heights and Ψ values. If we place linear, parallel lower bounds on the measurements in Figure 5, we can express β mathematically as a function of Ψ , for different ranges of H:

$$\begin{array}{ll} H < 200 \text{ m:} & \beta = 0.9091\Psi - 8.0^\circ \\ 200 \text{ m} < H < 300 \text{ m:} & \beta = 0.875\Psi - 3.75^\circ \\ H > 300 \text{ m:} & \beta = 0.8421\Psi - 0.68^\circ \end{array}$$

5.2.2.4 Rockfall range described in terms of the angle from the block to the talus peak

In the past, $\alpha = 25^\circ$ has been used as a rule of thumb for calculating how far rockfall can reach beyond the talus toe. This result is too inaccurate for practical application. The measurements indicate that this angle is geometrically dependent on the height and length of the talus, and that one of these parameters should be used together with α to describe rockfall range. As it appears today, the talus is

the result of the local topography and the rockfalls which have built the talus since the Ice Age. The topography of the mountainside and the transition to the terrain below governs the deposition of the falling blocks. This results in taluses of varying shape and size. Consequently, the talus peak does not provide a reliable reference for studying rockfall range.



Ratio between the talus height, H_2 , and α

This survey consists mostly of measurements where a talus has been developed, i.e. where there has been a certain amount of rockfall activity. The measurements are presented in Figure 8, where the values of α are related to the height, H_2 , of the talus. As we see, the measurements show a large spread with talus height, and naturally enough, the greatest spread is found with small taluses. This is because rockfall range is governed by factors other than the height of the talus. If we are to use α for describing the run-out, it is necessary to use a bound that includes all the measurements, in order to include the rockfalls that reach farthest. For measurements where the talus is below 50 m high, the spread of the measurements is 15° on either side of the mean value. The lower bound for α values related to the height of the talus is represented by a stippled line on Figure 8, and can be expressed as:



$$\alpha = 0.562H_2 + 13.76^\circ$$

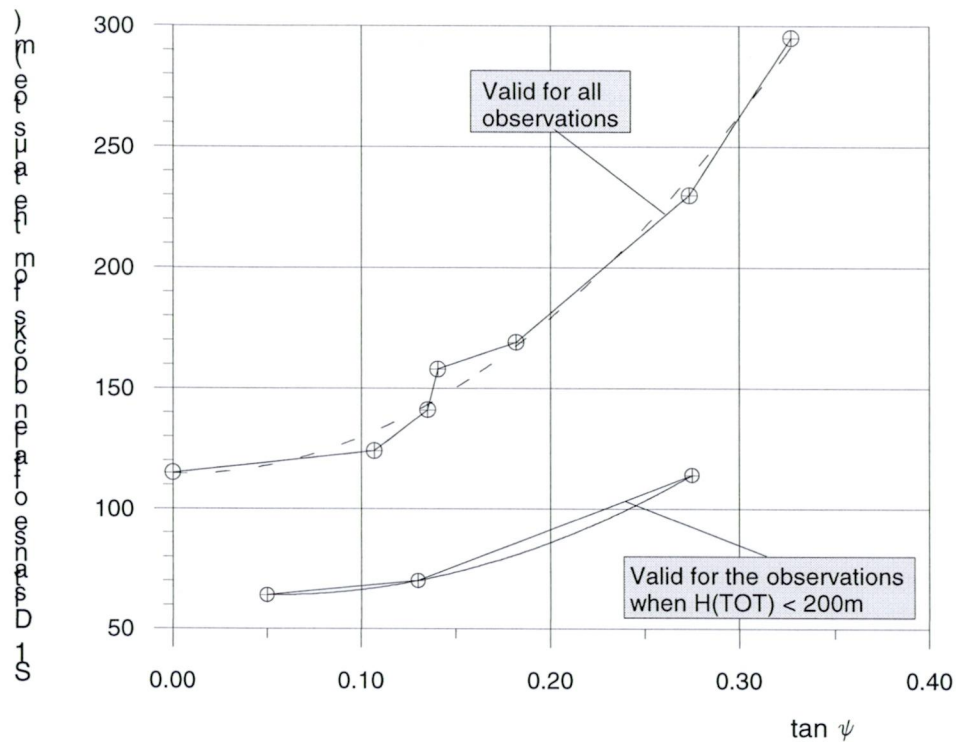
As shown on the figure, the α - angle with the longest run-out is less than 25° for taluses less than 200 m high. With taluses that are not higher than 100 m, α angles of down to 16° have been observed. The smallest α - angle for large taluses ($H_2 > 250$ m) is $\alpha = 27^\circ$. There are so few observations with such large taluses, that some reservations must be made regarding these results.

5.2.3 The significance of a steep run-out area beyond the talus toe

The results of the measurements show clearly that steep terrain beyond the talus toe is one of the most important factors governing rockfall range. However, this type of data has proved the most difficult to collect during fieldwork. In addition, these blocks lie so far out from the foot of the mountain that their origin could be moraine material. Fieldwork has shown that moraine blocks that have been transported for short distances are indistinguishable in shape from rockfall blocks. The measurements of blocks in steep run-out areas therefore all stem from recorded incidents of slides. The measurements provide reference values for what we know today about long rockfall run-outs, and thus constitute important empirical data which can be used in practical applications.

The measurement with the longest run-out recorded up to the present is for a block which reached 295 m beyond the talus toe from a 500 m high mountain-side, with an average slope between talus toe and block of 18.1° . The measurements show a marked increase in run-outs when the terrain slope beyond the talus exceeds 15° . Although we are short of measurements on this point, it looks as though particularly long run-outs may occur when the terrain slope, γ , is greater than 20° .

For all the measurements, the relationship between the terrain slope beyond the talus toe and the range beyond the talus toe has been considered. The longest run-outs are related to the slope γ and are presented in the figure below. The figure shows that the terrain slope appears to have a particularly great effect when the terrain beyond the talus toe is steeper than 15° . When the terrain slopes beyond the talus toe approach 20° , the results seem to indicate that particularly long run-outs are possible. We see from the figure that a range of 150 m is achieved in terrain with a slope of 6° , 200 m is attained with a slope of 13° , and approximately 300 m with a slope of 18° .



Range related to slope of the terrain beyond the talus toe.

An attempt has been made to group the measurements according to the height of the mountainside. It was not easy to find any clear correlation for the highest mountainsides. Only with lower mountainsides ($H < 200$ m) was it clearer that the height of the mountainside played an important part. In the preceding figure, the maximum ranges for $H < 200$ m are marked relative to the corresponding γ values. The shape of the curve is the same as for the higher mountainsides, but less markedly rounded in steep run-out areas. This tells us that blocks must have a high velocity as they pass the talus toe in order to attain long run-outs, and that the average resistance to rolling is probably higher than $\tan\gamma$, (γ -terrain inclination). For terrain slopes of 20° , $\tan(20^\circ) = 0.36$. For practical purposes it has been assumed that the resistance to rolling (f) of large blocks is of the order of 0.52 (Hung and Evans, 1989). Experiments are required to show whether this value can be applied in practice. However, it is clear that the resistance to rolling depends on the shape and size of the blocks and the quality of the substrate. In future work, it will be natural to investigate these factors. A polynomial fit was made for the line valid for all measurements:

$$S_1 = 115\text{m} + 19 \tan\gamma (90 \tan\gamma - 1)\text{m}, \quad (\text{coeff. of determ.}$$

$$R \text{ squared} = 0.99147)$$



5.2.4 Summary of empirical results for practical use

The results of the Norwegian survey of rockfalls are intended to be an aid in determining the probable maximum rockfall range from mountainsides subject to rockfall. All the results from 155 single cases studied can be used in correlating a given mountain-side, in particular when a mountainside has normal features. It is of vital importance to comply with the limitations of the empirical equations, especially the γ -limitations. The results of the survey that can be applied in practice are listed as follows:

- 1) Range (S_1) related to the height of the mountainside (H_{TOT}):

$$S_1 = 0.3065H_{TOT} + 24.1 \text{ m (applies to 98\% of the measurements, } \gamma < 12^\circ)$$

- 2) The range measured in terms of the angle (β) from the fallen block to the top of the uppermost scarp of the mountainside:

$$\beta \geq 31^\circ, \quad (\text{when } 100 \text{ m} < H_{TOT} < 350 \text{ m, } \gamma < 12^\circ)$$

β increases with H_{tot} and:

$$\beta \geq 35^\circ, \quad (\text{when } 350 \text{ m} < H_{TOT} < 650 \text{ m, } \gamma < 12^\circ)$$

- 3) The range measured in terms of β and related to Ψ (the angle from the talus toe to the top of the uppermost scarp on the mountainside):

$$\beta = 0.9091\Psi - 8.0^\circ, \quad (\text{when } H_{TOT} < 200 \text{ m, } \gamma < 12^\circ)$$

$$\beta = 0.8750\Psi - 3.75^\circ, \quad (\text{when } 200 \text{ m} < H_{TOT} < 300 \text{ m, } \gamma < 12^\circ)$$

$$\beta = 0.8421\Psi - 0.68^\circ, \quad (\text{when } H_{TOT} > 300 \text{ m, } \gamma < 12^\circ)$$

- 4) The range related to the talus peak in terms of angle α (the angle from the block to the talus peak):

$$\alpha = 0.0562[H_2] + 13.76^\circ, \quad (H_2 \text{ is the height of the talus, } \gamma < 12^\circ)$$

The expression does not apply to small and only slightly developed taluses. Consequently this relationship must be used with caution.

- 5) The range beyond the talus toe (S_1) expressed by the angle of the terrain beyond the talus toe:

$$S_1 = 115\text{m} + 19 \tan\gamma(90 \tan\gamma - 1)\text{m}, \quad (\text{when } H_{TOT} < 650\text{m, } \gamma < 20^\circ)$$

This expression is valid for all mountainsides in the investigation, but there can be found another expression for mountainsides lower than 200m.

These equations is valid for steep terrain outside the talus toe, but still within the limitation of $\gamma < 20^\circ$.

5.2.5 Formulas used in hazard zoning

The NGI approach for empirical calculation of rockfall range in hazard zoning is based on three assumptions that is applied in each calculation.

1) First our measurements show that the inclination from the block to the uppermost scarp is larger or equal to 30° .

2) Next the model calculates the runout with the formulae

$$S_1 = a \cdot H + b = 0.3065H_{TOT} + 24.1 \text{ m}$$

if the terrain outside the talus toe is gentler tha 12° .

3) If the terrain outside the talus toe is steep, that is steeper than 12° , we use a different formulae:

$$S_1 = 115\text{m} + 19 \tan\gamma (90 \tan\gamma - 1)\text{m}$$

where the average steepness of the terrain is used. The model makes the calculations after a profile is drawn manually on the digital map. The talus toe is defined by an angle (25°) that is, where the steep part of the talus ends. It is understood that this map calculation has to be investigated in the field. The results on the map can be seen on a profile and saved on a file or printed for further work.

5.3 Debris flows.

5.3.1 Starting zones

Debris flows are triggered either in an existing river channel in periods with high runoff, or by slumps and slides from the side slopes reaching into the channel creating instability. All slopes steeper than 30° are potential hazards zones. Drainage basins having a short hydrological response time, with steep unstable side slopes are most subjected to debris flows. Debris slides are most likely to occur along terrain depressions where water concentrates. Soil structure and texture also play an important role on the degree of hazard, as debris flows normally have their slip surface along the relatively impermeable

layer at 0,5-1,0 m depth with high content of clay and silt. The overlying layer has a higher permeability due to roots, animal and frost action.

The stability of the slope therefore depends largely on shear forces acting along this sliding plane, and not on the tensile strength of the soil. Most debris flows occur in spring and autumn associated with periods of rapid snow melt or heavy rain, and often a combination of both. Excess porewater pressure increases shear stress along the potential sliding surfaces, and decreases shear resistance. Both these factors have a negative effect on slope stability.

The aspect of the slope plays an important role on stability, as west facing slopes in the maritime climate of the west coast of Norway receive greater precipitation than leeward slopes due to the orographic effect from prevailing westerly winds. In addition, the largest amounts of snowmelt are produced in south and west facing slopes, due to higher wind speeds and more intense solar radiation in these slopes. The importance of these two factors is clearly demonstrated by the fact that most failures occur in slopes facing from south to west (Gregersen and Sandersen, 1989).

In Norway, there has been a growing tendency that debris flows are triggered by human disturbance of the natural conditions:

- Changing of the drainage, for example along forest roads, in steep terrain
- Extensive logging

In the first case the problem arises in combination with blockage of the culverts in periods with heavy runoff and abundant material transport. Erosion at the foot of steep cuttings can create sliding into the drainage channels. One should therefore closely plan the drainage system when new forest roads are under construction in steep terrain.

Logging affects the stability of the slope in two ways. Firstly, the water content of the soil will normally increase due to the removal of the water consuming trees. Secondly, the anchoring effect of the root system will be reduced. Both these factors have a negative effect on slope stability. Extensive logging in steep terrain overlying residential areas should therefore be avoided.

5.3.2 Runout distance

The runout of debris flows are mainly dependant on:

1. Volume of the sliding material
2. Water content of the sliding material



3. Degree of confinement in the runout zone.

Most of the material involved in the debris flow becomes entrained by erosion downstream of the point of initiation. In the runout zone the coarse grain sizes (blocks and stones) are accumulated first, and successively finer and finer sediments are accumulated through the runout zone. One should however be aware of the ability of the debris flows to transport big boulders far out into the runout zone. In areas with frequent debris flow activity, large debris fans have developed at the foot of the hillsides.

Dynamic equations for runout have been developed, for example by Takahashi (1981). The runout, X (m) from the upper point of the sedimentation area can be expressed by:

$$X = V^2 / G$$

$$V = v_i \cos (\theta_i - \theta_u) [(1 + gh_i \cos \theta_i) / 2 v_i^2]$$

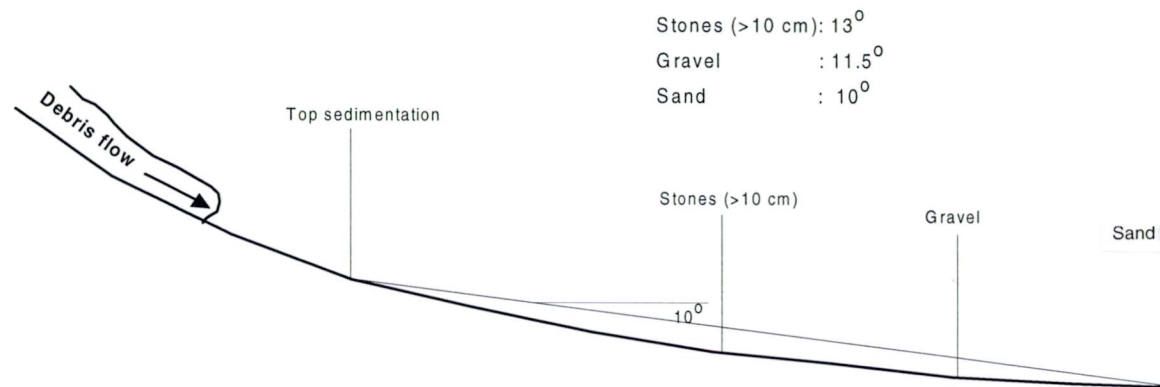
$$G = g(S_f \cos \theta_u - \sin \theta_u)$$

v_i , h_i and θ_i refer to the velocity, flow height and slope gradient in the section above the sedimentation area, whereas v_u , h_u and θ_u refer to the velocity, flow height and slope gradient at the entrance of the fan. S_f is the friction coefficient of the flowing material.

The most important factors governing the runout in this model are:

- The gradient in the runout zone
- The flowing depth
- The friction coefficient of the flowing material

Runout distance and velocity profile of the flowing material can also be calculated by granular flow models. The dynamics of debris flows are complex, involving both fluid and soil mechanics (Harbitz, 1996). The limited amount of real events makes it hard to evaluate and calibrate the existing models.



Runout distance of debris flows by topographical factors

In Norway, runout estimates are mostly based on empirical and topographical models. The runout can be estimated by the inclination of the straight line connecting the runout with the point in the track where sedimentation is the predominant process. This point of sedimentation usually coincides with bed inclination of 15⁰ in confined and 20⁰ in unconfined channels. Stones with diameter greater than 10 cm can reach down to 13⁰, while the sand fraction can go as far as 10⁰, see the figure above.

The volume of the sliding material is probably the most important factor for the extent of the runout zone. If several millions of m³ is involved, the runout can not be evaluated by simple dynamic or topographic models. This is especially important if large rivers are blocked and huge amounts of water are dammed with the possibility of generation of catastrophic flood waves downstream.

5.3.3 Identification of debris flow hazard

Evidence of earlier debris flow activity can be identified by terrain formations; ravines indicating erosion in the upper part and fan shaped accumulations at the foot of the hillside. Blikra (1997) has developed a method which makes it possible to evaluate the frequency of debris flows by studying the matrix of the sedimentary facies. The deposited material is studied in test pits, and by C¹⁴ datings of the organic material it is possible to estimate slide frequency during the different climatic periods since the last ice age. Each hazard has a specific matrix, and if different hazards are involved, these may be identified by this method.

5.3.4 Debris flow hazard zoning

Mapping of debris flow hazard involves two main evaluations:

- The hydrological regime of the drainage basin



- The availability of sediment sources
- The stability of the river channel on the entrance of the runout zone

Drainage basins responding quickly on rainfall or snowmelt input are most dangerous. Lakes or gentle inclined wetlands will store water and lead to elongated flow hydrographs, while steep basins with less water storage capacity will have more concentrated hydrographs and higher debris flow activity. The largest sedimentation fans are normally associated with the last category of drainage basin. Models for estimation of hydrological response can be used to evaluate runoff of different recurrence intervals.

The debris flow activity is highest in rivers which have abundant steep and unstable side slopes. Geomorphological maps will give valuable information on the extent of sediment sources within the drainage basin. Field inspection of these locations is needed to evaluate the stability and the quantity of potential sediment supply.

The spreading of the material into the fan area depends to a large degree on the stability of the river channel. Deep incised channels with stable side slopes will prevent lateral spreading. In shallow and unstable channels the possibility for lateral spreading is much higher. Only careful field inspection can give answer to this problem.

6 CASE STUDY OF NATURAL HAZARD ZONING

6.1 Main aim.

The aim of the case study was to study a small, populated area subjected to different natural hazards as snow avalanches, debris flows and rock falls. The output of the study is a map where the actual hazards were presented as a hazard zone map according to the safety requirements of the Norwegian Building and Planning act, as described in sect. 4.5. According to these regulations, three different hazard zones is shown on the hazard map.

The hazard zones are identified as lines that limit the hazard zones:

| <u>Building type</u> | <u>Hazard line/Frequency per year</u> | <u>Color of line</u> |
|----------------------------|---------------------------------------|----------------------|
| Garages, simpler buildings | 10^{-1} | Red |
| Dwelling houses | 10^{-3} | Green |

In addition, a line that shows the frequency of the $3 \cdot 10^{-3}$ slide hazard is included in the map. The reason for this intermediate line, or hazard zone, is that the Building Regulations requires a minimum safety at the $3 \cdot 10^{-3}$ level when a dwelling house is going to be rebuilt because of fire damage or extensive increase of living area.

It is important to note that the Norwegian Building regulations use the return periods of avalanches and slides as a basis for the regulations. It is stated in the text of these regulations that buildings, or its nearest surroundings should not be endangered by avalanches of the given frequency. Hence the building regulations does not take into account the total risk, as risk is defined as the product of probability (i.e. frequency of an avalanche), times the consequences of the avalanche. Consequently, the risk of death is therefore not an explicit subject in the Norwegian Building Regulations. The hazard maps that are developed in Norway are accordingly «Natural Hazards Frequency Maps», not «Natural Hazards Risk Maps».

6.2 Location, topography and climate of the study area.

The area chosen for the study is the village of Geiranger, a small farming and tourist village at the inner end of the Geiranger fiord, in the community of Stranda, county of Møre og Romsdal, in western Norway.





The area studied has a stretch of 7 kilometers, located in a steep valley, with 5 different settlements between the fiord level and 420 m a.sl. Geiranger is surrounded by mountains mainly to the northeast and southwest. The mountains ascend directly from the fiord level to 1600-1700 m a. sl., see map Appendix 1.

Most of the mountains that surround the village have slopes steeper than 30°. Much of the terrain consist of bare rock faces, especially in the upper parts of the slopes. The lower parts are mostly covered by morainic deposits, or by loose material transported downhill by numerous snow avalanches, rock falls and debris slides.

Average monthly and yearly precipitation rates for Geiranger in mm:

| Jan | Feb | Mar | Apr | May | Jun | Jul | Aug | Sep | Oc | Nov | Dec | Year |
|-----|-----|-----|-----|-----|-----|-----|-----|-----|-----|-----|-----|------|
| 168 | 116 | 99 | 63 | 56 | 65 | 91 | 99 | 132 | 123 | 141 | 115 | 1248 |

The average yearly precipitation is 1248 mm, spring is the driest period, autumn has most abundant precipitation.

Normally the precipitation rate during 3-5 days will be decisive for the release of snow avalanches. The precipitation during the last 24 hr period prior to the release, is most important, both for snow avalanches and for debris slides.

Maximum observed precipitation (mm), during a 24 hr period is measured to:

| Jan | Feb | Mar | Apr | May | Jun | Jul | Aug | Sep | Oct | Nov | Dec |
|-----|-----|-----|-----|-----|-----|-----|-----|-----|-----|-----|-----|
| 65 | 50 | 46 | 69 | 36 | 43 | 44 | 62 | 63 | 74 | 73 | 62 |

There is a tendency for the maximum levels to be somewhat lower during the summer and spring periods than the autumn level. The winter maximum is about 50-74 mm per day, corresponding to a snow fall of 50-75 cm. Usually big snow avalanches are triggered after snow falls of 75-100 cm in 3-5 days. The winter recordings clearly show that snow avalanches may occur in the area.

Experience indicates that 24 hr precipitation rates of 8% of the average yearly rainfall is necessary for the release of debris slides. The equivalent water supply may also be caused by snow melt. Normally, debris slides in the area are triggered as the result of heavy rain in combination with warm winds and snowmelt.

Climatic analyses from The Norwegian Meteorological Institute indicates that Geiranger will experience precipitation rates of 125 mm per 24 hrs, with a probability of 1/1000 per year. This level represent 10% of the yearly average.



6.3 Recorded avalanches and slides in Geiranger

The recorded avalanches in Geiranger dates back to 1796, a time span of 200 years. Only the major avalanche accidents, or avalanches that have been a threat to human life or buildings are recorded. All the numerous avalanches which have occurred in the uninhabited parts of the area are omitted. Most of these avalanches are not even recorded by the local public.

Information of historic avalanches and slides are gathered by interviewing the local public, especially elderly persons who have great local knowledge. In addition, written information from local news papers, local history literature, police reports, and church archives are used. A detailed description of the avalanches are given by Domaas et al. (1997). A total of 38 major avalanche incidents, located to 24 avalanche paths, are recorded since 1796, see map Appendix 1. This is an average of a major snow avalanche accident every 5-6 year in Geiranger. The recordings indicate a time span from 2-3 years, up to 20-30 years between the avalanche accidents.

During these years, 13 people have been killed by snow avalanches, 5 heavily injured. 47 dwelling houses destroyed or serious damaged, likewise 6 barns and about 40 other buildings. Numerous road closures are reported, and several cases of damaged electric powerlines and telephone lines.

In Geiranger, many areas are exposed to both rock falls and different types of earth slides. The most common type of earth slides are the debris flows which usually is connected to the rivers and brooks in the area. Rock falls may also induce debris flows as by the impact on slopes covered by loose deposits. The Geiranger area was covered by ice up to 9500 y. before present. Most of the debris flows is probably younger than 3500 years, because of a dryer climate prior to this time.

The historic records of debris flows date back to 1885, and 15 major accidents of debris slides are reported. Damage have been done to farm land, roads, bridges and houses. No reports on severe human casualties are reported.

The rock fall hazard is found first of all in vertical cliffs northeast of the town to a height of 300m a.s.l. It is thought that the rock falls are evenly distributed with time, when a long term scale is applied.

Of the three hazard types in Geiranger: snow avalanches, debris flows and rock falls, snow avalanches are the dominating hazard, debris flows holding the second position.



7 GIS AS A TOOL FOR HAZARD ZONING.

7.1 General

Digital maps and computerbased runout calculations have been in operation in avalanche hazard zoning at NGI since 1982, when the Digital Terrain Model TERMOS was developed at the institute. (Toppe and Lied 1984, Toppe 1987). The basis for the computerbased hazard zoning was the digital maps in scale 1:50.000 which were developed by the Norwegian Geographical Survey from the beginning of the 1980-ies.

7.2 Hazard zoning by GIS

During the last years NGI has applied a commercial available GIS system for avalanche hazard evaluations. The GIS system is used in combination with a commercial Digital Terrain Model (DTM).

The GIS system used by NGI is Pumatstation GIS (PS - GIS), a geographical information system with Microsoft Windows user interface, which have been developed in close cooperation with Norwegian users. The system has a general SQL interface which enables the connecting of data from external databases to digital map data. Both raster and vector data may be used. Standard picture files and scanned paper maps can be used as background for vector information. Vector data may be imported from SOSI, DXF or WMF format files. The GIS system is integrated with other MS Windows based programmes. The system runs on Pentium PC's of standard capacities.

Each avalanche and slide path is drawn on the computer in its maximum known extent, and given a name and identification number. The runout calculations are performed by using the SURFER DTM system which is an accurate and easy accesible commercial DTM, with an accuracy well within the needs of runout calculations.

By the Surfer programme all areas steeper than 30° are calculated automatically. These «steep» areas is regarded as the potential starting zones for snow avalanches, rock falls and debris slides.

The topographical runout models described in section 5, is programmed into the GIS system on the vectorized digital maps. By this way the potential runout distance may be calculated along defined avalanche paths.

The procedure for runout calculations is described in section 2 also.

Information of every avalanche and slide is collected in a relation database. (Excel) The database may be activated from the map by pointing at the actual

avalanche or slide at the computer screen. The database contains topographical and climatical conditions connected to the avalanche or slide incidents, date and place of incident, damage done, and source of information. The database will be connected to a national database on properties (GAB-database; Streets, Adresses and Buildings), where details on the actual property, such as owners identity, size and type of property etc. are registered.

The hazard zones are compiled according to the national safety regulations described in section 4. Examples of the hazard zone maps are included in Appendix 1.

8 REFERENCES

Azimi C., Desvarreux P., Giraud A., Martin Cocher J. 1982. Methode de calcul de la dynamique des chutes de blocks. Application a l'etude du versant de la montagne de la Pale (Vercors). Bull. liaison Labo P. et Ch. 122, pp. 93-102.

Azzoni, A. 1993. Methods for predicting rockfalls. Dept. of Geol. Imp. College of Sci., Tech. and Med., Univ. of London.

Banks D.C. & Strohm W.E. 1974. Calculations of rock slide velocities. Advances in Rock Mechanics. Proc. 3rd Congr. Int. Soc. Rock Mech., vol. 2B, Denver. pp.187-195.

Borel G. 1991 Proceedings of a workshop on avalanche dynamics 14-18 may 1990. Mitteilungen des Eidgenössischen Institut für Schnee- und Lawinenforschung. Juli 1991. Nr. 48. Edited by H.U. Gubler.

Bosco G. & Mongiovi' L. 1986. Analisi dei meccanismi di rottura per crollo e progetto degli interventi di protezione. Atti XVI Convegno Naz. Geotecnica, Bologna, vol III, pp.197-204.

Camponuovo G.F. & Fumagalli E. 1977. ISMES experience on the model of St. Martino Proc. Meeting on Rockfall dynamics and protective works effectiveness, Bergamo. publ. ISMES no 90. pp.25-39.

Decoudres, F., Zimmermann, T. 1987. Three dimensional dynamic calculation of rockfalls. Proc. 6th Int. Congress on Rock Mechanics, pp. 337-342.

van Dijke, J.J. & van Westen, C.J. 1990. Rockfall hazard: a geomorphological application of neighbourhood analysis with ILWIS. ITC-journal no.1.

Domaas, U. 1985. On rockfall range. NGI-report 585000-1. (in norw.)

Domaas U. 1994. Geometrical methods of calculating rockfall range. EU-project: «Meteorological factors influencing slope stability and movement type».

Domaas U., Blikra L., Sandersen F., Lied K., 1997. Geiranger. Natural Hazard Zone Maps. NGI report 964035-1, March 1 1997. (In Norwegian)

Falchetta J.L. 1985. Etude cinématique et dynamique de chute de blocks rocheux, Thesa, INSA, Lyon.

Gregersen, O. and Sandersen, F. 1989: Landslide: Extent and significance in Norway. In Landslides: Extent and Economic Significance, Brabb & Harrod (eds)

Gubler H. 1990. Proceedings of a workshop on avalanche dynamics 14-18 may 1990. Mitteilungen des Eidgenössischen Institut für Schnee- und Lawinenforschung. Juli 1991. Nr. 48. Edited by H.U. Gubler.

Hacar B., Bollo F., Hacar R. 1977. Bodies falling down on different slopes. Dynamic studies. Proc. 9th Int. Conf. Soil Mech. Found. Eng. Vol 2, Tokyo, pp. 91-95.

Harbitz C. 1996. Computational models for rock slide and debris flow motion. Norwegian Geotechnical Institute, report 585910-6.

Harbitz C. 1996. Computational modelse for dense snow avalanche motion Norwegian Geotechnical Institute, report 581250-3.

Harbitz C. 1997. A survey of computational models for snow avalanche motion. Norwegian Geotechnical Institute, report 581220-1.

Hoek E. (1987). A program in Basic for the analysis of rockfalls from slopes, Unpubl.

Hungr O., & Evans S.G. 1988 Engineering evaluation of fragmental rockfall hazard. Proc. 5th Int. Symp. on Landslides, Lausanne, pp.685-690.

Hungr, O. & Evans, S.G. 1989. Engineering aspects of rockfall hazards in Canada. Thurber Consultants, Vancouver, B.C.



Hestnes E. 1990. Norwegian Demands on Avalanche Safety - Legislation, Quality Policy and Judicial Practice. NGI-report 581000-4, 6. november 1990.

Hestnes E. , Lied K 1980. Natural-Hazard maps for land-use planning in Norway. Journal of Glaciology, Vol.26,No.94, 1980.

Hestnes E. & Schieldrop B. 1977. Full scale tests on rockfall with calculations. NGI-report 54702-2.

Hopf J. (1990) Proceedings of a workshop on avalanche dynamics 14-18 may 1990. Mitteilungen des Eidgenössischen Institut für Schnee- und Lawinenforschung. Juli 1991. Nr. 48. Edited by H.U. Gubler.

Johannesson T., Jonasson K., Fridgeirsdottir K., (1996) A topographic model for Icelandic avalanches. Icelandic Meteorological Office, Internal report VI-G 96003-UR03.

Jonasson K., Arnalds T. (1997). A Method for Avalanche Risk Assessment. Vedurstofa Islands Report VI-G97036-UR28

Kirby, M.J. & Statham, I. (1975). Surface stone movement and scree formation. Journal of Geology, Vol.83, p.349-362.

Larsen, J.O. & Schieldrop, B. (1989). Rockfall test at Støren by the road E6 (02.11.89) with
theoretical evaluations and calculations. NGI-report 585000-6.

Larsen J.O. (1993). Rockfall simulation models and their practical application. Univ of Colorado at Boulder. Dept. of Civil, Architectural and Environmental Eng.

Paiola A. (1978). Movimenti franosi in Friuli. Comportamento dei corpi che cadono su un pendio e calcolo del limite di espansione potenziale. Technica Italiane. No 6.

Paronuzzi P. (1989). Probabilistic approach for design optimization of rockfall protective barriers. Quarterly J. Eng. Geol. London. Vol. 22. pp.135-146.

Pfeiffer T.J. & Bowen T.D. (1989). Computer simulation of rockfalls. Bull. of Ass.of Eng. Geol. Vol. XXVI, No 1. pp. 135-146.

Piteau D.R & Clayton R. (1977). Disc. of «Computerized Design of Rock slopes using interactive graphics for the input and output of geometrical data» by Cundall P.A., Voegele M.D. & Fairhurst C. Proc. 16th Symp. on Rock Mechanics pp. 62-63



Salm B. (1990) Proceedings of a workshop on avalanche dynamics 14-18 may 1990. Mitteilungen des Eidgenössischen Institut für Schnee- und Lawinenforschung. Juli 1991. Nr. 48. Edited by H.U. Gubler.

Scheidegger, A.E. (1973). On the prediction of the reach and velocity of catastrophic landslides. Rock Mechanics 5 p.231-236. Springer Verlag.

Scheidegger, A.E. (1975). Physical aspects of natural catastrophes. Elsevier scientific pub. comp.

Schildrop B. 1977. Models for calculation of dynamical behaviour of rockslides. Fjellsprenningsteknikk, bergmekanikk, geoteknikk 1997. Conference in Oslo, Norway.

Schildrop B. 1987. Rullende steinblokkers forsering av beskyttelsesvoller belyst ved en forenklet modell. NGI-report 585000-2.

Schildrop B. 1988. Mangelanters bevegelse på skråplan. NGI-report 585000-4.

Schildrop B. 1990. Theory for calculation of maximum rock jump lengths. NGI-report 585000-8.

Spang R.M. & Rautenstrauch R.W. 1988. Empirical and mathematical approaches to rockfall protection and their practical application. Proc. 5th Int. Symp. on Landslides, Lausanne. pp. 1237-1243.

Toppe R. 1987. Terrain models---A tool for natural hazard mapping. Avalanche Formation, Movement and Effects (Proceedings of the Davos Symposium September 1986). IAHS Publ. no. 162, 1987.



Appendix 1 - Hazard zone maps for Geiranger